Defense Nuclear Agency
Alexandria, VA 22310-3398

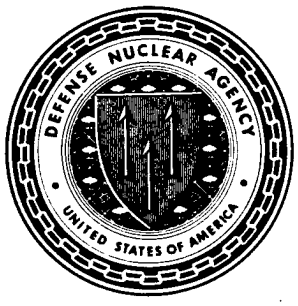

DSWA-TR-96-81

Development of an Improved Direct Neutron Sensor

Francis E. LeVert
K.E.M.P. Corporation
1725 East Magnolia Avenue
Knoxville, TN 37917

November 1997

Technical Report

CONTRACT No. DNA 001-90-C-0082

DESTRUCTION NOTICE:

Destroy this report when it is no longer needed.
Do not return to sender.

PLEASE NOTIFY THE DEFENSE SPECIAL WEAPONS AGENCY, ATTN: CSTI, 6801TELEGRAPH ROAD, ALEXANDRIA, VA 22310-3398, IF YOUR ADDRESS IS INCORRECT, IF YOU WISH IT DELETED FROM THE DISTRIBUTION LIST, OR IF THE ADDRESSEE IS NO LONGER EMPLOYED BY YOUR ORGANIZATION.

DISTRIBUTION LIST UPDATE

This mailer is provided to enable DSWA to maintain current distribution lists for reports. (We would appreciate your providing the requested information.)

NOTE:
Please return the mailing label from the document so that any additions, changes, corrections or deletions can be made easily. For distribution cancellation or more information call DSWA/IMAS (703) 325-1036.

☐ Add the individual listed to your distribution list.

☐ Delete the cited organization/individual.

☐ Change of address.

NAME: _____

ORGANIZATION: _____

OLD ADDRESS	CURRENT ADDRESS
_____	_____
_____	_____
_____	_____

TELEPHONE NUMBER: ( ) _____

DSWA PUBLICATION NUMBER/TITLE	CHANGES/DELETIONS/ADDITIONS, etc.) *(Attach Sheet if more Space is Required)*
_____	_____
_____	_____
_____	_____

DSWA OR OTHER GOVERNMENT CONTRACT NUMBER: _____

CERTIFICATION OF NEED-TO-KNOW BY GOVERNMENT SPONSOR (if other than DSWA):

SPONSORING ORGANIZATION: _____

CONTRACTING OFFICER OR REPRESENTATIVE: _____

SIGNATURE: _____

CUT HERE AND RETURN

DEFENSE SPECIAL WEAPONS AGENCY
ATTN: IMAS
6801 TELEGRAPH ROAD
ALEXANDRIA, VA 22310-3398

DEFENSE SPECIAL WEAPONS AGENCY
ATTN: IMAS
6801 TELEGRAPH ROAD
ALEXANDRIA, VA 22310-3398

REPORT DOCUMENTATION PAGE

Form Approved
OMB No. 0704-0188

1. AGENCY USE ONLY (Leave blank)	2. REPORT DATE	3. REPORT TYPE AND DATES COVERED
	971101	Technical 900916 - 960927

4. TITLE AND SUBTITLE
Development of an Improved Direct Neutron Sensor

5. FUNDING NUMBERS
C - DNA 001-90-C-0082
PE - 63224C
PR - SF
TA - SB
WU - DH00093

6. AUTHOR(S)
Francis E. LeVert

7. PERFORMING ORGANIZATION NAME(S) AND ADDRESS(ES)
K.E.M.P. Corporation
1725 East Magnolia Avenue
Knoxville, TN 37917

8. PERFORMING ORGANIZATION REPORT NUMBER
KB-FR-14

9. SPONSORING/MONITORING AGENCY NAME(S) AND ADDRESS(ES)
Defense Special Weapons Agency
6801 Telegraph Road
Alexandria, VA 22310-3398
WEL/Kim

10. SPONSORING/MONITORING AGENCY REPORT NUMBER
DSWA-TR-96-81

11. SUPPLEMENTARY NOTES
This work was sponsored by the Defense Special Weapons Agency under RDT&E RMC Code B7664D SF SB 00093 PRPD 1950A 25904D.

12a. DISTRIBUTION/AVAILABILITY STATEMENT
Approved for public release; distribution is unlimited.

12b. DISTRIBUTION CODE

13. ABSTRACT (*Maximum 200 words*)

The feasibility study of the use of conductive polymers to design and assemble a neutron monitor sensitive to fast and thermal neutrons has been completed. Polyacetylene, polypyrrole and polythiophene conductive polymers with conductivities that range from 10^{-4} $(\Omega\text{-cm})^{-1}$ down to 10^{-11} $(\Omega\text{-cm})^{-1}$ were used in this investigation. The sensors were exposed to neutrons from an Am-Be sealed source with an average energy of 2.5 MeV and a 14 MeV neutron generator.

The conductive polymer film was inserted between two structural elements consisting of quartz plates of polyethylene prisms with electrode structures formed with conductive paints or other conductive materials interposed between the polymer structural elements.

The polyacetylene film used in the investigation exhibited the most consistent results revealing a sensitivity of ~10^{-15} coulombs/neutron/cm^2. A polyacetylene based directionally sensitive detector with parallel plate geometry exposed to 14 MeV neutrons revealed a two-to-one front-to-back directional discrimination capacity. In tests where the sensors that were designed with isotropic sensitivity were exposed to 100 microcurie Am-Be source, thick BF_4 doped and undoped sensors revealed a minimum sensitivity of ~400 n/cm^2 (nv-thermal), when referenced to a calibrated Boron lined proportional counter with a minimum sensitivity of 12 n/cm^2 (nv-thermal).

14. SUBJECT TERMS			15. NUMBER OF PAGES
Neutrons	Polythiophene		66
Fast Thermal	Direct Detection	Polypyrrole	
Polyacetylene	Conductive Polymers	Neutron Sensor	16. PRICE CODE

17. SECURITY CLASSIFICATION OF REPORT	18. SECURITY CLASSIFICATION OF THIS PAGE	19. SECURITY CLASSIFICATION OF ABSTRACT	20. LIMITATION OF ABSTRACT
UNCLASSIFIED	UNCLASSIFIED	UNCLASSIFIED	SAR

NSN 7540-280-5500

Standar d Form 298 ((rev. 2-89)
Precribed by ANSI Sta. 239-18
298-102

CLASSIFIED BY:

N/A since Unclassified.

DECLASSIFY ON:

N/A since Unclassified.

SUMMARY

The feasibility study of the use of conductive polymers to design and assemble a neutron monitor sensitive to fast and thermal neutrons has been completed. Polyacetylene, polypyrrole, and polythiophene conductive polymers with conductivities that range from 10^{-4} $(\Omega\text{-cm})^{-1}$ were used in the investigation. The sensors were exposed to neutrons from an Am-Be sealed source with an average energy of ~2.5 MeV and a 14 MeV neutron generator.

The sensors were designed for charge generation by direct proton-neutron interactions in the polymer and by indirect ionization with recoil protons from interactions in polyethylene prisms on each of the opposing surfaces of the polymer. Several sensors with directional sensitivity and some with isotropic detection sensitivity were designed and built for testing during this effort.

The conductive polymer film were inserted between two structural elements consisting of quartz plates or polyethylene prisms with electrode structures formed with conductive paints or other conductive materials interposed between the polymer structural elements. Results are presented that suggest that a properly designed conductive polymer based sensor can be made sensitive to fast and high energy neutrons. In keeping with the results of Phase I, the polyacetylene film exhibited the most consistent results revealing a sensitivity of ~10^{-15} coulombs/neutron/cm^2. A polyacetylene based directionally sensitive detector with parallel plate geometry exposed to 14 MeV neutrons revealed a two-to-one front-to-back directional discrimination capacity. In tests where the sensors that were designed with isotropic sensitivity were exposed to a 100 microcurie Am-Be source, thick BF_4 doped and undoped sensors revealed a minimum sensitivity of ~400n/cm^2 (nv-thermal), when referenced to a calibrated Victoreen Model 488A Boron lined proportional counter with a minimum sensitivity of 12 n/cm^2 (nv thermal).

The measurement results reported here were conducted with standard laboratory equipment and with a prototype monitor constructed as a part of the Phase II effort. The prototype monitor consisted of a very low noise FET input charge preamplifier, pulse shaping circuitry, a single channel analyzer (SCA) and a LCD counter.

In temperature tests of the polymers in which polyacetylene, polypyrrole and polythiophene were cooled from 80°C down to -10°C, the conductivity decreased with decreasing temperature in a well behaved manner. From ~21°C to -10°C, the conductivity varied from $2x10^{-11}$ down to $6x10^{-13}$ $(\Omega\text{-cm})^{-1}$.

These results suggest that a neutron sensor based on the use of polyacetylene or other polymers produced with good quality control can be constructed and made sensitive to high and low energy neutrons.

TABLE OF CONTENTS

TABLE OF CONTENTS (CONTINUED)

FIGURES

TABLES

SECTION 1
BACKGROUND

All existing neutron detectors utilize inferential (indirect) techniques to measure neutron fluxes[1,2]. The work of Butler[3] with conductive polymers suggested the possibility of a new class of neutron sensors that could be configured in large sizes and various shapes. The Phase I results obtained by K.E.M.P. Corporation and the work of Butler showed that when polyacetylene, with an initial conductivity of ~10^{-10} $(\Omega\text{-cm})^{-1}$, was exposed to neutrons there was an increase in conductivity of the polymer which varied linearly with increasing neutron fluence. The linear increase in the conductivity was attributed to the creation of reactive sites caused by the removal of protons from the monomers in the polymer chains. These reactive sites, in the presence of a reagent, behave similarly to electron accepting dopant atoms; that is, they act to effectively increase the dopant concentration in the material.

This neutron bombardment has the opposite effect on the conductivity of some doped semiconductor materials. In these materials, the concentration of dopants decreases with increased neutron fluence. The reduction in dopant concentration as a function of neutron fluence has been observed by several investigators[4,5] in doped silicon and other semiconductor materials (e.g. GaAs). In these materials, proton and neutron irradiation cause cluster defects, resulting from the recoil of the silicon atoms in silicon-based semiconductor materials. These cluster defects result in defect energy levels that are as effective as electron trapping centers in both n– and p-type materials, thereby inducing carrier removal. The removal of carriers causes an increase in the resistivity and a corresponding decrease in the conductivity of the material. This change in conductivity is temporal as is the case in most radiation damaged materials. Kania et. al.[6] recently employed this neutron-induced doping reduction effect in GaAs as a means of developing an ultra fast responding neutron detector. This detector concept relies on the modulation of the detector's conductivity by energetic ions that generate electron-hole pairs in the bulk

GaAs. Since the neutron induced change in the conductivity of the film in this investigation is also temporal, this effort was designed to investigate whether a sensor based on this concept can be deployed as a high energy neutron detector. The neutron-proton interactions in the polymer create free carriers plus electron-hole pairs via ionization by the recoil protons. The electron-hole pairs and the free carriers in the polymer have a finite lifetime which depends on the mobility of carriers and electron-hole pair recombination time. Thus, the response time of the detector will be governed by these parameters.

This Phase II is a continuation of the work done by KEMP in the Phase I investigation. In Phase I, the conductivities of the selected polymers ranged from a high of 10^{-3} $(\Omega\text{-cm})^{-1}$ down to 10^{-9} $(\Omega\text{-cm})^{-1}$. The polymer films were exposed to a fast neutron flux of $1.2\text{x}10^{9}$ n/cm^2-sec from six Cf-252 sources for 2, 4 and 10 days. The neutron irradiation studies conducted on the polyacetylene showed that the sensitivity of its conductivity to neutron fluence was $\sim 10^{-23}$ $(\text{-cm})^{-1}/n/cm^2$. The sensitivity of the conductivity of the copolymer poly(pyrrole-co-N-methylpyrrole) doped with BF_4 to neutron fluence was measured to be $\sim 10^{-22}$ $(\text{-cm})^{-1}/n/cm^2$. These results suggested that the lower the conductivity of the polymers the greater the sensitivity to neutron fluences. It provided the basis for the Phase II Objectives discussed in Section 2.

SECTION 2

PROJECT OBJECTIVES

The technical objectives of this Phase II effort were to:

1. **Establish the energy resolution/discrimination capability and lower limit of detectability of source neutrons using a polymer based neutron sensor.**

2. **Demonstrate technical feasibility of using conductive polymers as the active element in a neutron sensor via the use of a neutron source such as Cf-252.**

3. **Fabricate and assemble one working prototype isotropic neutron sensor.**

4. **Determine the sensitivity of the isotropic neutron sensor to 14 MeV neutrons and neutron fields with an average energy of 2 MeV(e.g., a Cf-252 neutron source).**

5. **Investigate neutron - sensor interaction physics for neutrons with energies as high 100 MeV.**

6. **Examine the feasibility of developing a directionally sensitive neutron detector.**

7. **Fabricate and assemble one directionally sensitive neutron sensor.**

8. **Experimentally determine the sensitivity of the directionally**

sensitive neutron detector to 14 MeV fission spectra neutrons.

9. **Examine the effect of different environmental conditions on the electrical and mechanical properties of the sensor materials.**

SECTION 3
THEORY

The chemistry and physics of conductive polymer materials have been discussed in numerous technical papers. This Phase II effort relates to their use as direct neutron detectors. Some of the basis for their use in this application can be found in the fact that effective dopant density in conductive polymers[5] has been experimentally shown to vary linearly with neutron fluence. It can be shown that the net dopant density after neutron irradiation of a conductive polymer may be written as:

$$N = N_o + a \text{ , dopants/cm}^3 \qquad (3.1)$$

where N_o is the initial dopant density and a is the effective electron acceptor generation rate caused by proton recoils due to neutron fluence. The quantity, a, in Equation 3.1, which is related to the neutron-proton interaction rate within the polymer was calculated in Phase I to be 1.2×10^{-3} proton/neutron-cms for Cf-252 neutrons impinging on a 0.05 mm thick polyacetylene film. Using Equation 3.1, the resistivity of the polymer can be represented by

$$\rho = \frac{1}{q\mu N} (\Omega - cm)^{-1} \qquad (3.2)$$

where q is the electron charge, μ the majority hole carrier mobility, and N the net dopant density as given by Equation 3.1. Using Equations 3.1 and 3.2, the current output of a detector based on the change in resistivity can be represented as

$$I = \frac{\gamma N V_o \mu q A}{\varepsilon L^2} , Amps \qquad (3.3)$$

With the exception of γ, V_o, A, Σ and L, all the quantities in Equation 3.3 are as previously defined. γ, V_o, A, Σ and L are the energy deposited in the film per liberated proton , the applied voltage, the cross-sectional area of the film, the energy required to form an ion pair, and its thickness, respectively. When this current is supplied to the input of a high impedance device, with impedance R, the output voltage can be represented by

$$V_{out}=\frac{\gamma N A V_0 \mu q R}{\varepsilon L^2}.Volts \qquad (3.4)$$

This relationship (i.e., Equation 3.4) gives the output voltage resulting from conductivity changes caused by n-p interactions that produce ionization in a conductive polymer based sensor.

SECTION 4

DESIGN OF A CONDUCTIVE POLYMER NEUTRON MONITOR

4.1 THE PHYSICAL AND ELECTRICAL CHARACTERISTICS OF THE CONDUCTIVE POLYMERS USED IN PHASE II.

The polymers used to assemble the sensor for examination of the feasibility of constructing a conductive based polymer neutron sensor consisted of trans-doped polyacetylene, undoped polyacetylene, polypyrrole and poly(3-octylthiophene) (P3OT). They had cross sectional areas of 25 cm^2 and thicknesses between 0.05 and 1 mm (see Table 4.1). The conductivity values given in Table 4.1 were the " as received" values measured by KEMP using the four terminal resistivity technique. All the values were within 10% of those indicated by the suppliers. The P3OT and polypyrrole are air stable polymers. The choice of polymers was based on the Phase I experimental and calculational results, where it was shown that the sensitivity of polyacetylene to neutron fluences varied inversely with the conductivity of the polymer. The Phase I results for polyacetylene showed that the sensitivity of its conductivity to neutron fluence was $\sim 10^{-23}$ $(\Omega\text{-cm})^{-1}/n/cm^2$. The sensitivity of the conductivity of the copolymer poly(pyrrole-co-N-methylpyrrole) doped with BF_4 was measured to be $\sim 10^{-22}$ $(\Omega\text{-cm})^{-1}/n/cm^2$. Polymers were selected that could be produced with conductivities between 10^{-3} and $< 10^{-11}$ $(\Omega\text{-cm})^{-1}$) with existing laboratory techniques. All of the polymers were supplied by the chemists at the University of Texas at Arlington and Dallas who supplied the Phase I polymers.

Table 4-1. Mechanical and Electrical Properties of Film Used in this Investigation.

Polymer	Thickness, mm	Area, cm^2	Dopant	Conductivity, $(\Omega\text{-cm})^{-1}$
Trans-Polyacetylene	≥0.1	~36	none	10^{-11}
Trans Polyacetylene	≥0.1	~36	BF_4	10^{-8}
Trans Polyacetylene	0.1	20	none	10^{-9}
Polypyrrole	.2	25	none	10^{-9}
Polypyrrole	.2 - 1	25	BF_4	10^{-5}
Polythiophene	0.1	25	none	10^{-9}
Polythiophene	0.1	25	BF_4	10^{-5}
Poly(3-octylthiophene (ABA Copolymer Blend/Polystyrene)	0.130	30	PF_6	10^{-9}

All of the film materials exhibited some undesirable physical characteristics that were due primarily to the production methods, chemical characteristics of the long chain polymers

and the fact that all of the materials were secured from university laboratories not set up for the production of commercial grade film materials. The derivative, poly(3-octylthiophene), was blended with 10% polystyrene to reduce its brittleness. However, it exhibited significant variation in its thickness with holes distributed randomly throughout several of the coupons. The holes resulted from uncontrolled deposition of the polymer on the substrate used to capture the material. The polypyrrole and polyacetylene exhibited extreme brittleness. All of the films were soaked in Acetonitrile (CH_3 CN) to reduce the brittleness during the assembly process.

4.2 ASSEMBLY OF ISOTROPIC POLYACETYLENE, POLYPYRROLE AND POLY(3-OCTYLTHIOPHENE) (P3OT) BASED SENSORS.

The active volumes of the neutron sensors that were used in the Phase II testing varied between 4 and ~6 cm in frontal area. The thicknesses of the film varied between .05 mm and ~2 mm. These sample sensors were primarily used in the early investigations of the materials. A schematic drawing of the sensor design is shown in Figure 4-1. Carbon electrodes were painted on each surface of a prism (i.e., quartz, polyethylene, etc.) that is proximate the film. Electrical contact with the carbon coated electrodes will be established using silver epoxy traces that are extended to the outer surfaces of the electrode plates where they make contact with external electrical leads. These systems were sealed with TORR SEAL^{tm} ceramic epoxy as shown schematically in Figure 4-1. The guard ring shown in Figure 4-1 was included to overcome stray current interference with the measurements. The epoxy, which is manufactured by the Kurt J. Lesker Co., was selected as a sealant because of its low vapor pressure and outgassing characteristics to avoid volatile components that might react with sites created by n,p reactions in the films. The film was soaked in CH_3 CN to reduce the brittleness during the assembly process.

Fourteen sensors similar in design to that of Figure 4-1 with an average area of 5 cm were fabricated for testing. Eight of the sensors had carbon-carbon electrodes with guard rings painted on the inner surfaces of the upper and lower electrode plates. Four of the

units had carbon-silver electrodes and two had silver-silver electrodes.

One variation of the electrode structure design consisted of conductive strips placed on the opposing edges of a film coupon. In addition to the quartz plates, several sensors were assembled with 1.27 cm thick polyethylene prisms with the electrode structure painted on opposing surfaces with either carbon paint or silver epoxy. The purpose of polyethylene prisms was to utilize the knock-on protons to generate charge in the polymer due to the ion

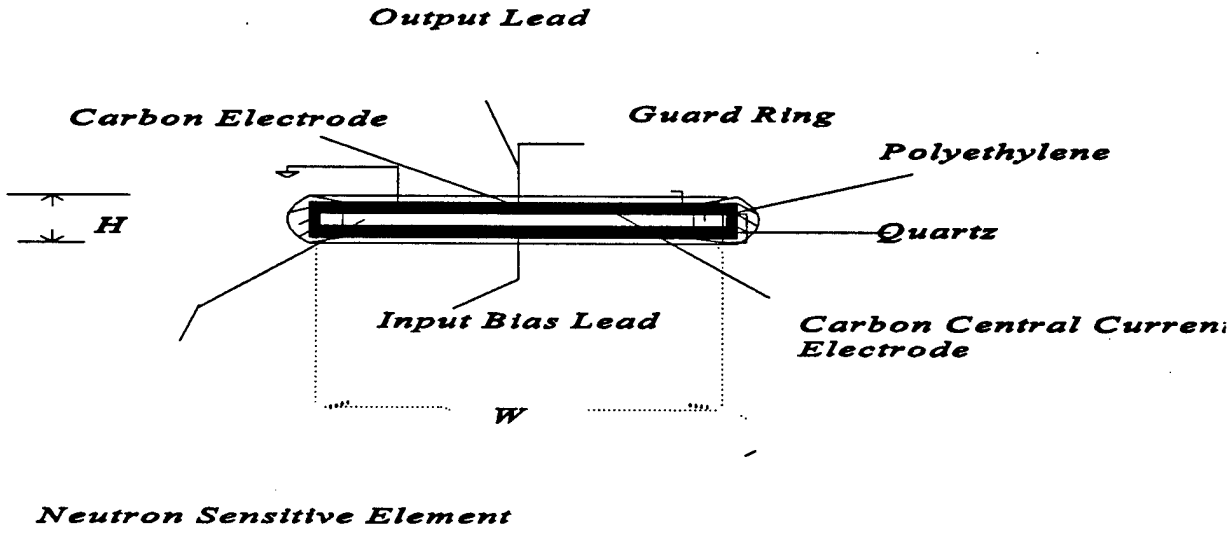

Figure 4-1. Essential Components of Assembled Neutron Sensor.

pairs produced in it by the protons impinging upon it. B.J. Moyer[9] has shown that the proton production for thin polyethylene radiators above a proton energy E_B corresponding to a radiator thickness "x" is given by Equation 4.1

$$\frac{N(E_b,x)}{\varphi(E_B)}=\frac{1}{2}\Sigma_H AR(E_n)\frac{x}{R(E_B)}\left[1+\frac{x}{R(E_n)}-\frac{9}{5}\left[\frac{x}{R(E_n)}\right]^{\frac{3}{2}}\right] \qquad (4.1)$$

where Σ is the macroscopic n-p scattering cross section of the target; E_B and E_n are the bias and incident neutron energies , respectively. The energy E_n corresponds to the maximum energy available to the recoil proton; A is the area of the radiator ; and R is the proton range in the radiator. He demonstrated that the ratio of proton production to the incident neutron flux varies linearly with the energy of the incident neutron over a range of energies between 1 MeV and ~ 7 MeV. For polyethylene radiator thicknesses between .37 mm and ~ 3 mm the proton producing efficiency production is essentially independent of the thickness of the radiator. Also, he found that the proton/neutron production efficiency varied between ~.08x10^{-3} to ~.8x10$^{-3,}$ over the 1 to 7 MeV neutron energy range as suggested by Equation 4.1. In the case of the polymers neutrons interact, for example, with the polyacetylene knocking protons out of the polyacetylene $(CH)_x$ and leaving behind a reactive site. The liberated protons also produce ion pairs within the polymer. Polyacetylene, with its high concentration of hydrogen, has a neutron mean free path for fission spectrum neutron energies of ~ 10 cm. For the undoped film with the thicknesses used in these investigation, this implies that for neutrons with an average energy of ~ 2 MeV less than 0.1% will undergo n-p reactions in the film. The reaction rate is somewhat lower for the polypyrrole and the polythiophene. From Equation 4.1, one observes that the proton yield of polyethylene is a linear function of the cross section of hydrogen; therefore; at very high neutron energies (i.e., > 40 MeV[10]), the efficiency of the thin polymers used in these measurements becomes essentially zero or ~0.01%. This fact made the use of the polyethylene radiators even more important for this feasibility study.

Shiraishi[11] et. al. estimated the proton production efficiency for a 100 micron thick polyethylene to be between ~$1x10^{-4}$ and $8x10^{-4}$ for 1.0 MeV and 11 MeV, respectively. Above 11 MeV the neutron - hydrogen drops off very rapidly. These facts were considered in the design of the thick polyethylene prism electrode sensors.

Since exposure to air (i.e. oxygen) results in uncontrolled changes in the conductivity of trans-polyacetylene, the sensors were assembled in a helium atmosphere and sealed with epoxy. All of the sensor designs were housed in a metallic enclosure. Even though the remaining polymers are stable in air they were also assembled in the inert atmosphere. A sketch of the prototype cylindrical sensor assembled for the Phase II testing is shown in Figure 4-2.

4.3 ASSEMBLY OF A DIRECTIONALLY SENSITIVE NEUTRON SENSOR.

In addition to the abovementioned sensor designs, a directionally sensitive sensor was assembled based on the design of a directionally sensitive neutron detector developed by the researchers of Reference 12 for use as incore fast neutron flux monitors. In this design KEMP juxtaposed a Tantalum plate next to the first surface of a polyacetylene coupon and a .5mm polyethylene radiator with a carbon coating on the face of the polyethylene facing the polymer. Proton recoils from the radiator provide directional sensitivity through the $\cos(\theta)$ dependent of the (n-p) scattering cross section.

Using the calculated results of Reference 12, for a pure neutron source field, the front-to-back sensitivity ratio was calculated to be ~4.3

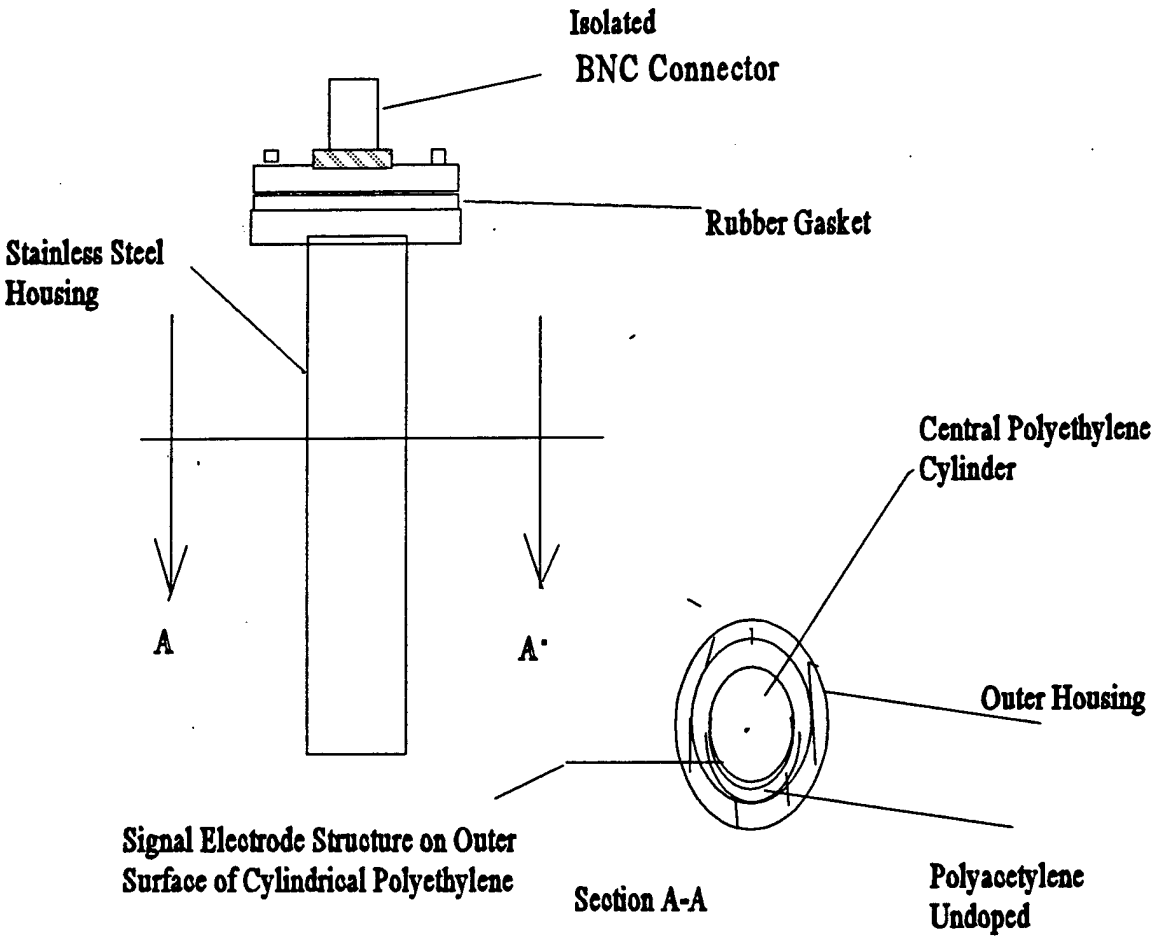

Figure 4-2. Sketch of a Prototype Sensor Used in Phase II Measurements.

SECTION 5
SIGNAL CONDITIONING ELECTRONICS

The initial preamplifier used in this Phase II effort was a voltage sensitive preamplifier. It has the advantage of faster rise time and a higher signal to noise ratio than a charge sensitive preamplifier. These advantages are overshadowed by the dependence of the pulse output of the voltage preamp on the capacitance and leakage resistance of the detector while the charge sensitive preamplifier is insensitive to the capacitance and leakage resistance of the neutron detector. This makes the charge sensitive preamplifier design better suited for the conductive polymer based sensors whose capacitance tends to be very low varying between ~10 and 50 pf.

5.1 PREAMPLIFIER/AMPLIFIER/SINGLE CHANNEL ANALYZER.

The charge - voltage converter shown in Figure 5-1 and Figure A-1 is the core of the detection unit. The PCB layout shown in Figures A-2 through A-3 are for the voltage preamplifier design. They have been modified with the addition of jumper wires to accommodate the charge sensitive preamplifier front end. Also, an inverting amplifier was added at the output of U3 for pulse polarity considerations. The main characteristics are:

1) A FET input stage;
2) A charge-voltage pre-amplifier with a charge gain of Q/C_f;
3) A pulse shaping amplifier and,
4) A single channel analyzer circuit whose output is fed directly to an LCD counter.

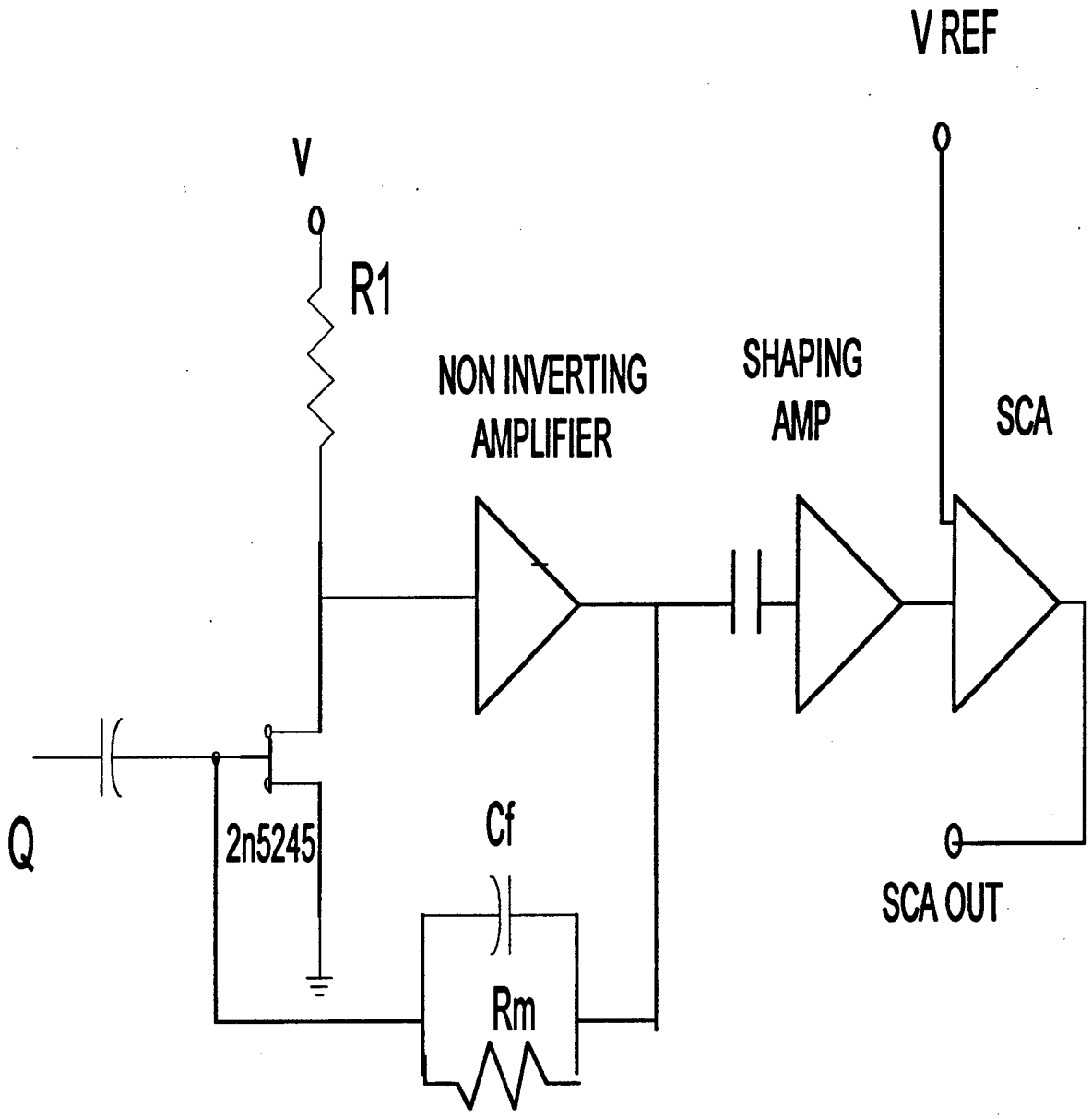

Figure 5-1. Schematic Representation of Charge Primp, Shaping Amplifier and SCA Circuit.

The FET input combined with the operational amplifier provides a very low noise signal input stage. The charge-sensitive preamplifier measures the quantity of charge collected by the detector. The charge Q released by the detector is a function of the energy deposited in the intrinsic region of the polymer and is given by

$$Q = Ee/\epsilon \tag{5.1}$$

where E is the energy of the incident radiation, e is the charge of an electron (1.602×10^{-19} C), and ϵ is the energy required to produce an electron hole pair in the active region of the polymer (between 2.50 and ~4.05 ev per ion pair). A block diagram of the preamplifier/amplifier/SCA circuit is shown by Figure 5-1. The charge-sensitive preamplifier measures the quantity of charge released by the detector by integrating the charge on the feedback capacitor C_f. For a charge Q released by the detector, the output pulse of the preamplifier has an amplitude V_o given by

$$V_o = Q/C_f \tag{5.2}$$

and the time constant is given by

$$\tau = R_f C_f \tag{5.3}$$

where R_f is the preamplifier feedback resistor.

The resulting preamplifier output "tail pulse" has a very short peak and an extremely long tail with time constant ~ 0.1 ms. The shape and amplitude of the preamplifier output pulse are not very practical for analyzing; therefore, it must be shaped and amplified. The output of the preamplifier is ac coupled to the shaping amplifier section of the circuit. The two-stage shaping amplifier has a nominal gain of 150x and a shaping time of 2 milliseconds. The shaping amplifier differentiates the preamplifier tail pulse. The

resulting output pulse is proportional to input tail pulse, but has a shorter resolving time.

From Equations 5.1 through 5.3, the total conversion gain of the preamplifier is given by

$$\frac{V}{E} = \frac{e}{\varepsilon C_f} G\eta \qquad (5.4)$$

where G is the gain of the pulse shaping circuitry and η is the number of electron volts per MeV. The remaining quantities are as previously defined. The shaping amplifier output pulses are discriminated by pulse height in the SCA section of the circuit. Pulse amplitude is compared to a pre-set voltage threshold. Every time the threshold is exceeded, the SCA output to the counter a pulse for counting. Pulses with amplitude below the pre-set threshold are discarded. The discriminator threshold setting was determined by the experiments described in Section 4.0 and is set at 0.150 volts.

The preamplifier/amplifier/SCA circuit is contained on a 5 cm x 7 cm double-layer printed circuit board (PCB). Detailed schematic drawings and parts lists are found in Appendix A.

5.2 POWER SUPPLY SYSTEM.

The voltage multiplier of the circuit consists of voltage set-up regulators and voltage inverting regulators to convert the battery voltage to regulated +6v, -6v, +5v and -100v supplies. The initial design of the voltage supplies included the capability of applying a bias to the conductive polymer materials used in the detector. Block diagram of the voltage multiplier circuit is shown in Figure 5-2. The circuit requires a minimum battery terminal voltage of 2.1 volts to begin regulation. Battery voltage is provided by two D-size batteries connected in series. Two Alkaline batteries in series will provide an initial voltage of 3.0 volts and have a capacity of 14,000 milliamp hours . After the circuit has

started to regulate, it will continue to regulate with a battery terminal voltage as low as 1.6 volts.

Two voltage step-up regulators and two voltage inverting regulators are used. Each regulator is contained in a small 8-pin IC chip. The regulators are small 8-pin CMOS IC chips manufactured by Maxim Integrated Products Inc. The battery voltage is stepped-up to a regulated +6v and +5v by U2 and U3 respectively. U2 also monitors the battery terminal voltage and provides a high signal if the voltage is above 2.2v. When the voltage drops below 2.2v, the battery status of U2 indicates "low." The voltage inverting regulators, U4 and U1, supply the -6v supply and -100v bias respectively. U4 converts +6v to a regulated -6v. U1 converts +5v to -100v high voltage (HV) neutron detector bias. A 10:1 transformer T6 (refer to voltage multiplier drawing in Appendix A for circuit schematic) is used to reduce the HV output of U4 o 1.2v for the regulation of output (VREF). To begin regulation of the HV bias, U1 requires a larger amount of current than U3 (+5v regulator) can supply. To provide the start-up power required, a zenner diode is used between the +10v supply and +5v supply. During start-up the +5v supply is drained by U1 trying to start regulation. The 5.6v zenner diode will supply the needed voltage until U1 starts regulating. When U1 is regulating the load on the +5v regulator is minimal and it will regulate at +5v. Then the zenner will turn off. Total power consumption of the voltage multiplier circuit is 490 mW. The voltage multiplier circuit is approximately 70% (ratio of input power to output power). For the above efficiency, one set of fresh batteries can operate the neutron monitor for approximately 54 hours.

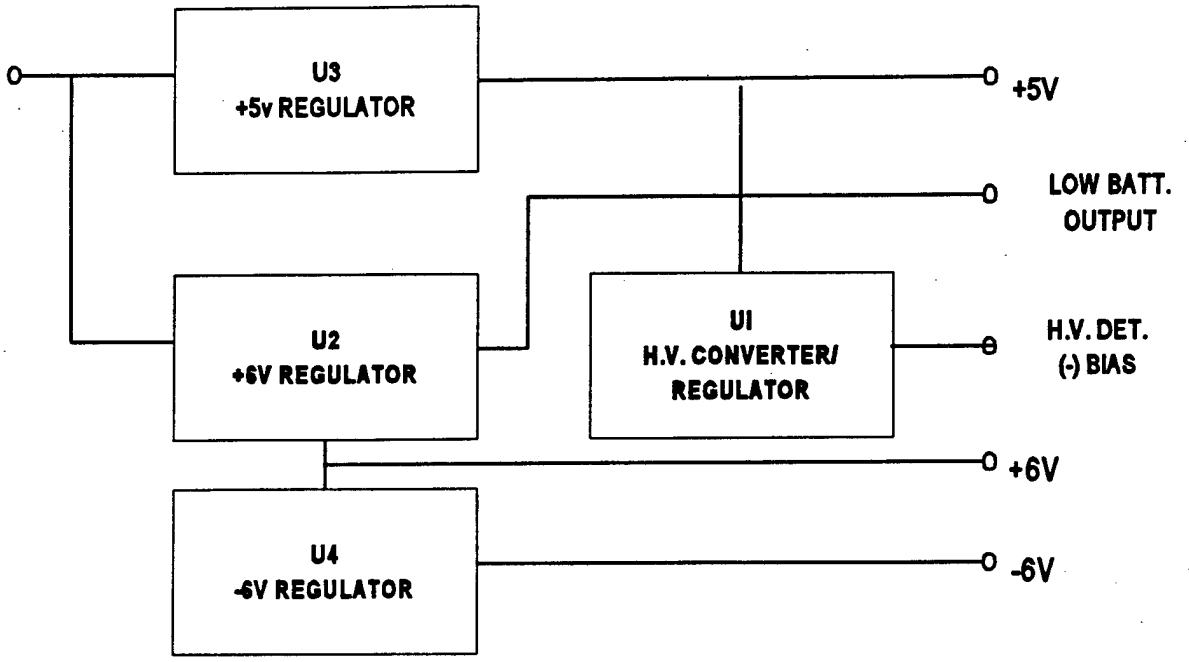

Figure 5-2. Block Diagram of the Voltage Multiplier.

5.3 ENCLOSURES FOR NEUTRON MONITOR.

The detector, preamplfier and signal conditioning electronics described in Section 5.1 are housed in a free standing MicroPak electronic instrument enclosure. The base/body is made of extruded aluminum. The design of the enclosure is given in Figure A-7 of Appendix A. The LCD counter is mounted on an end panel opposite the end where the detector is mounted as shown schematically in Figure 5-3. Its characteristics are shown schematically in Figure A-8 of Appendix A. The counter has to be manually started and stopped. It provides an integral number of counts accumulated over a given period of time.

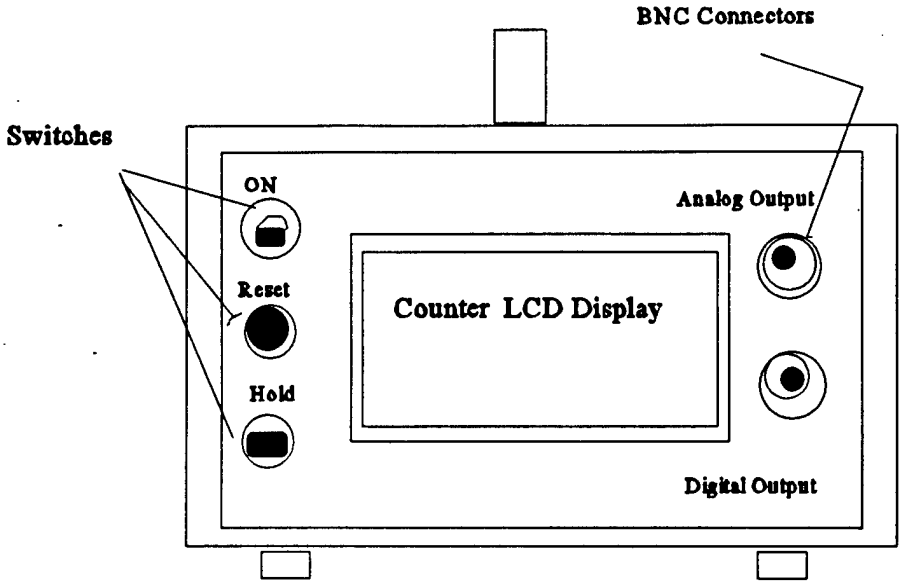

Figure 5-3. Schematic Representation Prototype Neutron Monitor.

SECTION 6

EXPERIMENTAL RESULTS

The neutron radiation testing was conducted in the radiation laboratory at KEMP's facilities and at the University of Kentucky. Tests were performed using a 100 microcurie Am-Be neutron source at KEMP's facilities and 14 MeV neutron generator at the University of Kentucky, Lexington, Ky 14 MeV neutron generator Laboratory. The generator is capable of producing $\sim 1x10^{11}$ neutron/second using a D-T reaction . The Am-Be neutron[14] source provides a source of neutrons whose energies are distributed as shown in Figure. 6-1. While the average neutron energy of the Am-Be is higher than that of CF-252, it had certain advantages that made it more easy to store at KEMP's facilities.

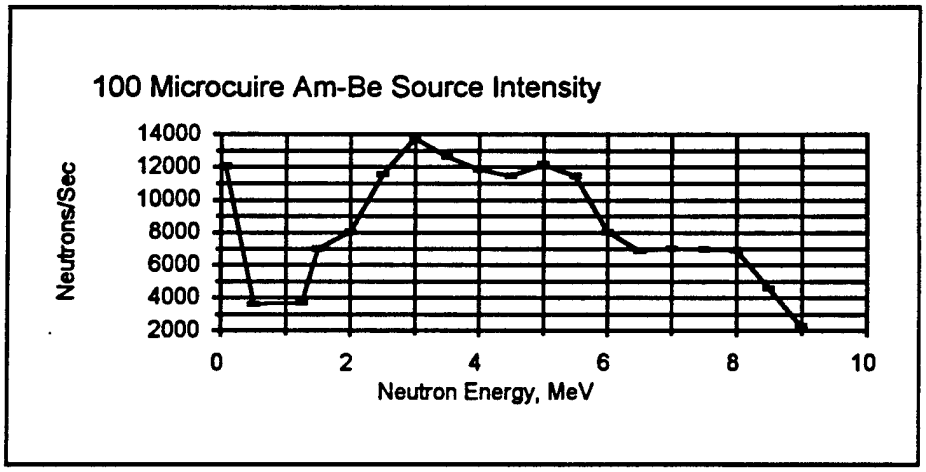

Figure 6-1. Am-Be Source Spectrum.

6.1 CHARACTERIZATION OF POLYACETYLENE, POLYPRROLE AND POLYTHIOPHENE BASED SENSORS USING A 100 MICROCURIE AM-BE SOURCE.

The neutron-hydrogen (n-p) interaction cross section is well known up to neutron energies of ~30 MeV[10]. The energy loss rate dE/dx for the recoil protons produced in an n-p reaction in organic polymers can be extrapolated from values for air using the Bragg-Kleeman Rule. Thus, if the energy required to create an ion pair within the polymers is known neutrons of various energies can be estimated. The purpose of these experiments was to estimate the amount of energy deposited in a polymer via the ionization process that would be required for the charge generated by a recoiling proton to be detectable in the presence of the inherent noise of these sensors. The polymer sensors were found to exhibit dark currents in the picoampere range. The RMS values of the dark currents were found to be comparable to values measured using a commercial Surface Barrier Detector. Trans-polyacetylene and polythiophene films with areas of approximately 4 cm^2 and conductivities of approximately 10^{-10} $(\Omega\text{-cm})^{-1}$ were the subject of experimental investigations. The purpose of these measurements was to determine whether the polymers would yield consistent and predictable results when exposed to a low intensity neutron source. Sensors were assembled with ohmic contacts (i.e. carbon-carbon electrodes) and exposed to a 100 microcurie Am-Be source. The experimental equipment consisted of the voltage preamplifier and composite amplifier whose output was fed to a data logger with a sampling rate of 30kHz and down loaded into a microcomputer for analysis.

During the measurements, the Am-Be source and the sensors were suspended in close proximity to the sensor (i.e., approximately 2 cm away from the sensor). Both polyacetylene and the polythiophene sensors were examined using the same experimental setup. Figure 6-2 shows a sample output time trace in which the polyacetylene sensor was attached to the input of the voltage preamplifier. The results in Figure 6-2 show the time dependent signals resulting from the collection of the charge created in the polymer by neutron-proton interactions and the inherent dark currents therein.

Pulses similar to these were used to establish the discriminator settings needed to prevent noise contamination of the measured neutron signals. In Figure 6-2, the RMS value of the sensor's dark current and the electronic noise was calculated to be .017 volts with peak-to-peak values of 50 millivolts. With the lower discriminator set at .050 volts, long term measurements suggested that the neutron interactions within the detector were calculated to be ~ 0.03 events/(seconds cm^2) or $1.25x10^{-4}$ events/neutron. The rise time of pulses typical of those shown in Figure 6-2, which averaged between four and five milliseconds, were used to set the resolving time of the voltage preamplifier and the time constants of the pulse shaping components of Figure 5-1.

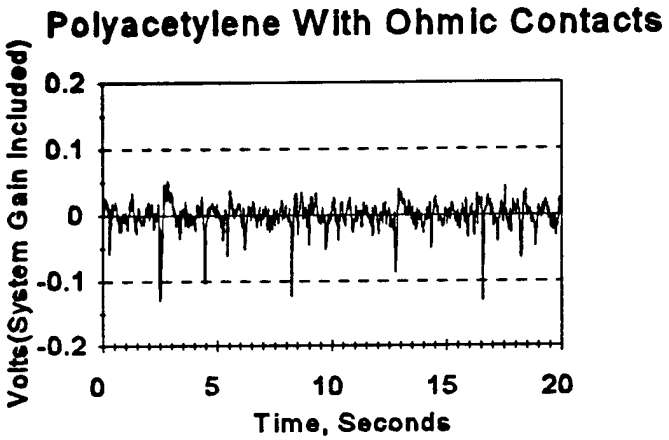

Figure 6-2. Response of Polyacetylene Sensor To Am-Be Neutron Source.

Figure 6-3 shows the response of a polythiophene based system. The polythiophene sensor results show a much higher noise level than that shown in Figure 6-2. When long term samples were

taken the signals were deconvoluted and the results used to calculate the effect of the circuit parameters (e.g., the RC time constants of the preamplifier and the sampling rate of the data logged) on the collection time of the charge generated in the polymer. The surface barrier detector (SB) tests were used in an attempt to understand the large noise component of the polyacetylene and polythiophene signals. The r.m.s. value of the SB noise signal was more than a factor of 2 lower than that measured for the PA and P3OT based sensors. The capacitances of the polymer detectors are more than a factor of 10 smaller than that of the surface barrier detector used in the comparison test (i.e., the capacitance of the surface barrier detector was ~ 47nF while the largest value measured for a multilayer polythiophene sensor was ~25 pf). Normally, the dark current is directly proportional to the capacitance of a detector. This fact suggested that there were other sources of the measured noise. These measurements were used, however, to establish the discriminator settings and gain of amplification stages of the signal conditioning electronics required to discriminate against noise during the neutron measurements.

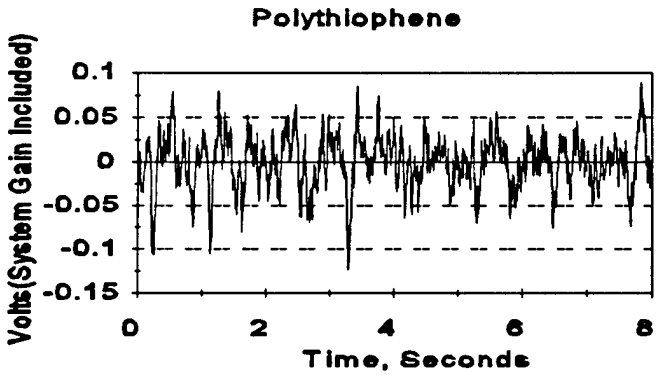

Figure 6-3. Response of Polythiophene Sensor to an Am-Be Neutron Source.

6.2 MOBILITY MEASUREMENTS.

Polymer films with planar electrodes made of combinations of tin-gold, indium-gold, silver-silver and carbon-carbon were used in the mobility measurements. The polymers used in the tests were trans-polyacetylene (PA), polythiophene (P3OT) and polypyrrole (PPY). The technical literature contains mobility estimates for polythiophene (PT) derivatives that vary between ~10^{-4} and 10^{-9} $cm^2/V\text{-}s$[16]. Published mobility values for PA and PPY vary as much as those of PT. The reported values vary considerably and depend on a variety of factors such as dopant concentration and method of fabrication. it was important that the mobility of the film used in this work be determined. Since the mobility of the majority carriers is related to the collection time for free charge liberated within the film, knowledge of it can be used in the design of the preamplifier and signal conditioning electronics.

Several experiments were performed in which the time-of-flight of holes (transit time) in the p-type, PT, PPY, and PA polymers were estimated. Polymers with thicknesses that varied between 60 - 250 μm were used. The electrodes were composed of paired quartz plates and polyethylene prisms with alternating high and low work function electrode combinations (i.e., relative to that of the polymer) mounted on the prisms. The mobility estimates were computed using the transit time of holes to the collecting electrode. The transit time[1] can be represented by

$$T = d^2/V\mu \qquad (6.1)$$

where V is the bias applied to or "built in " the sensor, μ is the mobility of the majority carriers and d is the thickness of the depletion zone. Values of V were measured for each sensor before each measurement and d was calculated using known parameters of the polymers. The quantity T is a transit time in the sense that it is the time required for holes to drift ~63%(1-1/e) of the way from their starting point to the edge of the depletion layer. Depending on the origin of the charge, the transit times can be expected to be distributed about a mean value. This mean value can be used to estimate the value of μ using Eq. 6.1.

A fast neutron flux (i. e., E ≥ 2.8 MeV) of ~ 300 n/cm²sec was imposed on the sensor. The interaction rate in the sensor was calculated to be between ~0.01 n/sec and.06 n/sec. With a low pass 3db point of 10kHz, the amplifier was capable of responding to pulses with transit times of ≤ 100 μs. The digital data logger was set to trigger on positive going pulses with amplitudes ≥ 10 MHz. The sampling rate was set at 1 MHz. Figure 6-4 shows the response of a PA polymer based sensor with a cross sectional area of ~ 2.25 cm² and a thickness of ~ 120 μm. The pulse in Figure 6-4 was sensed at the output stage of the voltage preamplifier and fed to the X-Y recorder. The voltage preamplifier was used because of its faster rise time. The output pulses were conditioned in the Keithley, digitized in the digital data logger and stored in the microcomputer. The increased rise time of the pulse in Figure 6-4 reflects the response time of the Keithley. Data recorded in the digital data logger for PT and PA based sensors was deconvoluted to remove the effect of the Keithley's response time and the signal conditioning at the digital data logger. When the data was deconvoluted the mean transit times, as defined above, were determined for both edge and planar electrode structure, using Weibull distribution functions. These mean values were used to compute the mobilities of the majority carriers for PT and PA as shown in Table 6-1.

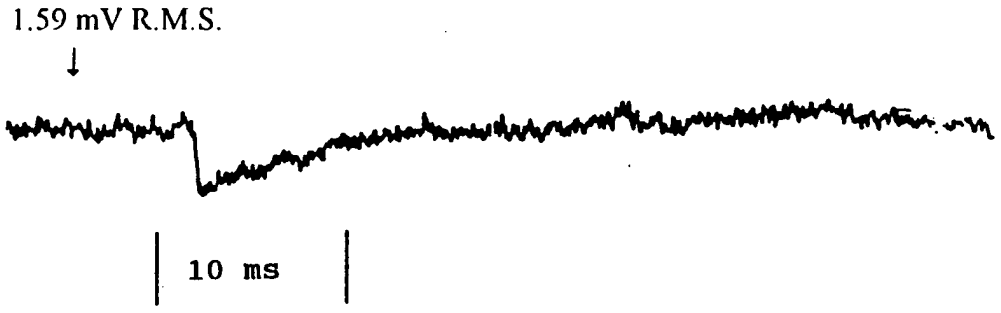

Figure 6-4. Output Pulse From Voltage Preamplifier Connected to a Polyacetylene Based Neutron Sensor.

Table 6-1. Electrical Parameters for Conductive Polymers Based on Neutron Sensor Studies.

	Vip	d [17,18],cm	μ(planar), $cm^2/(V-s)$	μ(edge), $cm^2/(V-s)$	σ $(\Omega-cm)^{-1}$
Polyacetylene	.016	$2.9x10^{-7}$	$3.26x10^{-9}$		$\sim10^{-10}$
Polyacetylene	.031	$2.9x10^{-7}$		$6.52x10^{-10}$	$2x10^{-10}$
Polythiophene (P3OT)	.121	$5.8x10^{-6}$	$2.5x10^{-7}$		$\sim10^{-9}$ - 10^{-11}
Polypyrrole	.3	---		---	10^{-7}

The calculated mobilities were much lower than that of holes in intrinsic silicon (~475 $cm^2/V-s$)[1] and those of P3Met($2.5x10^{-4}$ $cm^2/V-s$)[4] and P3HT (10^{-5} $cm^2/V-s$). However, the value computed for P3OT was approximately one order of magnitude less than the value computed by Fang et.al.(Reference 3) for P3OT of $3.53x10^{-9}$ $cm^2/V-s$. The conductivity values in Table 4-1 were determined using the expression where N_a is the carrier density, q the electronic charge and μ

$$\sigma = N_a q \mu \qquad (6.2)$$

the calculated mobility. The calculated conductivities agreed very well with the values reported by the film suppliers. These results suggest that the charge collection times for these polymers may be very long (i.e., compared to typical solid state detectors).

6.3 HIGH ENERGY NEUTRON EXAMINATION OF THE NEUTRON SENSORS.

The high energy neutron irradiation measurements were conducted at the Radioanalytical Service Facility at the University of Kentucky. The experimental setup included a Kaman Model A-

1250 neutron generator, one current and one voltage signal conditioning circuit that were separately connected to the sensors used in the measurements. The Voltage signal conditioning circuitry was coupled to the sensors by a charge-to-voltage converter with a response time of 10 ms. The polyacetylene based sensors show the most sensitivity to the neutron flux. The average sensitivity of the polyacetylene based sensors was calculated to be ~5.94×10^{-15} coulombs/neutron. All of the measured voltage values given in Table 6-2 are the average of at least two measurements in which the beam current of the generator was reduced to zero then increased back to 3 mA. Since the neutron yield of the generator is directly proportional to the beam current, it was expected that the measured voltage should vary essentially linearly with beam current as was demonstrated by the results in Table 6-2. Because of the setup at the University of Kentucky, which is not geared for this type of measurement, the position of the sensors relative to the target may have varied as much as 4-5 cms making a sensor-to-sensor comparison difficult.

The measurements of the direct modulation of the conductivity of several sensors using the circuit described above exhibited some inconsistencies (See Table 6-3). For example, the PT and PPY did not respond to the 14 MeV neutrons and the polarity of the measured current flowing through a sensor changed when it was exposed to neutrons. The initial currents {i.e. at zero beam current) were consistent with those measured when 100 volts were applied to the sensors during prior resistivity measurements. The measured currents for a triple layered sensor (sensor #3) were typical of those measured when a 100 VDC was applied to a sensor in the neutron field. The measured results for beam currents of 0, 0.85 and 3 milliamperes were 51, -500 and -1760 picoamperes, respectively. At the present time, there are no plausible explanations for the reversal in polarity of the measured currents.

Table 6-2. Response of Isotropic Polyacetylene Based Neutron Sensors to 14 MeV Neutrons.

Sensor Identification Number	Total Film Thickness, cm	Detector Bias, Volts	Electrode Stroture Painted on Quartz	Neutron Generator Beam Current, ma	Measured Output Voltage, Volts
1	0.0412	100	Carbon-Carbon	0 1 2 3	.06 1.84 3.2 4.4
2	.045	100	Carbon-Carbon	0 1 3	.09 2.42 4.91
5	.136	100	Carbon-Carbon	0 3	.2 7.66
20	.124	100	Carbon-Carbon	0 3	.10 5.99
2[b]	.099	100	Carbon-Silver	0 3	.15 3.80
10	.169	100	Carbon-Silver	0 3	.2 5.0
10[a]	.169	0	Carbon-Silver	0 3	.07 .6

a. Sensor #10 measured with no DC bias applied.

b. Film Doped with BF_4^-

The sensor with the largest response was removed and the housing containing the electronics was exposed to the beam to determine whether or not the observed signal was the result of interactions of non ionizing radiation (i.e., the electromagnetic fields associated with the generator's power supply). With the unit powered. the output signal revealed no dependence on the power level of the generator.

Table 6-3. Neutron (14 MeV) Modulation of Sensors Conductivity.

Central Electrode Resistance Between Parallel Electrodes, Megohms	layers of polymer	polymer	Electrode Material/Electrode Conductive Material	Out Current, Picoamps	Generator Beam Current,mA	Film Type
5	single	Undoped	Quartz/Carbon	+14 -47	0 3	P3OT/ Sensor #13
6.2	Triple	Undoped	Quartz/Carbon	51 500 1865	0 1 3	PA/ Sensor # 3
5.06	Triple	Doped	Polyethylene/Silver-Carbon	0 250 872	0 2 3	PA Sensor # 11
0.14	Double	Doped	Poltethylene/ Silver	-5.66 -6.1	0 3	PPY

6.4 HIGH ENERGY NEUTRON TESTS OF THE DIRECTIONAL SENSITIVITY OF A POLYACETYLENE BASED SENSOR.

The multi-plate sensor described in Section 4.3 was exposed to the 14 MeV neutron source. The device was positioned in a vertical position and irradiated with the generator current set at 3 mA for approximately one minute to allow for transient behavior. After each irradiation the sensor was rotated through 90° and the measurement repeated. The detector exhibited a front (i.e., with the polyethylene facing the neutron source) to back (i.e,. Tantalum facing the source) ratio of approximately 2 to 1 with the largest variation in signal current occurring when the edges of

the detector were in a plane that was normal to the surface of the neutron generator target. In these measurements, the output of the sensor was coupled directly to the input of a Keithley 610 picoammeter that was positioned such that it could be read from a location.

6.5 THE EXPERIMENTAL INVESTIGATION OF THE RESPONSE OF POLYACETYLENE, POLYPYRROLE AND POLYTHIOPHENE SENSORS TO AN AM-BE SOURCE.

The Am-Be source has a certified yield of ~$2x10^5$ neutrons per second. The examination of the response of the prototype neutron monitor with doped and undoped polyacetylene film coupons mounted between parallel polyethylene prisms and with film material mounted on a cylindrical polyethylene rod between two 0.1 mm thick Indium electrodes (See Figure 4-2) was conducted to determine the sensitivity of the device to low intensity neutron flux fields. Figure 6-1 shows the neutron energy spectrum of the Am-Be source. Thermal and fast neutron measurements were made with the prototype monitor along with two calibrated NIST traceable neutron survey meters (a Ludlum Model 15 and a Victoreen Model 488A). The Victoreen unit minus its polyethylene moderator was used to monitor the thermal neutron flux while the Ludlum unit complete with its moderator was used to monitor the fast and thermal neutron flux at the location of the prototype. All three instruments were mounted on the top of the neutron source shield. The source consists of a 40 centimeter diameter cylindrical container approximately 65 centimeters in height. The shield contains a 5 centimeter hole in a borated paraffin shield through which the source was moved up into a polyethylene cave where the neutrons were thermalized. Once the source was in the pure polyethylene shield, it was translated vertically in 5 centimeter intervals. The polyethylene cave is approximately 28 cms in height. After each movement the survey meters and the prototype neutron monitor were read. The fast neutron measurements were conducted with the source suspended in air and moved in 5 centimeter increments in a vertical direction toward the monitors. Figure 6-5 shows the responses of the prototype monitor, the Ludlum and Victoreen survey meters as the source was moved through the polyethylene cave into the air above the instrument in 5 cm increments. The was completely out of the cave at the 30 cm position on Figure 6-5. The neutron sensor in the monitor contained a

doped (BF_4) polyacetylene sensor. The results in Figure 6-5 are the counts per second per cm^2 area of the survey meters and the prototype for the average of ten three minute runs for each measurement point. These results suggest that the efficiency of the polymer based sensor with thick (1.27 cms) polyethylene prisms with electrodes painted on their inner surface is approximately 1-3% of that for a Boron lined bare proportional counter(i.e. the Victoreen model 488A counter). The Model 488A has a sensitivity as low as 12 thermal neutrons per square cms or approximately 0.045 mrem per hour. This fact would suggest that a polyacetylene based sensor surrounded by polyethyline prism (1.27 cm thickness) has a minimum sensitivity of 400 n/cm^2. Typical event rates in the neutron survey meters and polymer based sensor with a mrem polyethylene moderator is given in Table 6-4. In Table 6-4, the source was suspended above the detectors and lowered downwardly toward the detectors in 5 cm increments and then held at each location as integral measurements were made in five minute intervals. When the polymer detector was suspended in air and the source moved vertically past the unit with the thick polyethylene electrodes it exhibited a similar behavior to that of the directional detector during its rotation through 360° (see Figure 6-6). The trough at ~8 centimeters corresponds to the vertical location where a horizontal plane that includes the center of gravity of the source also contains the vertical center of the polymer sensor.

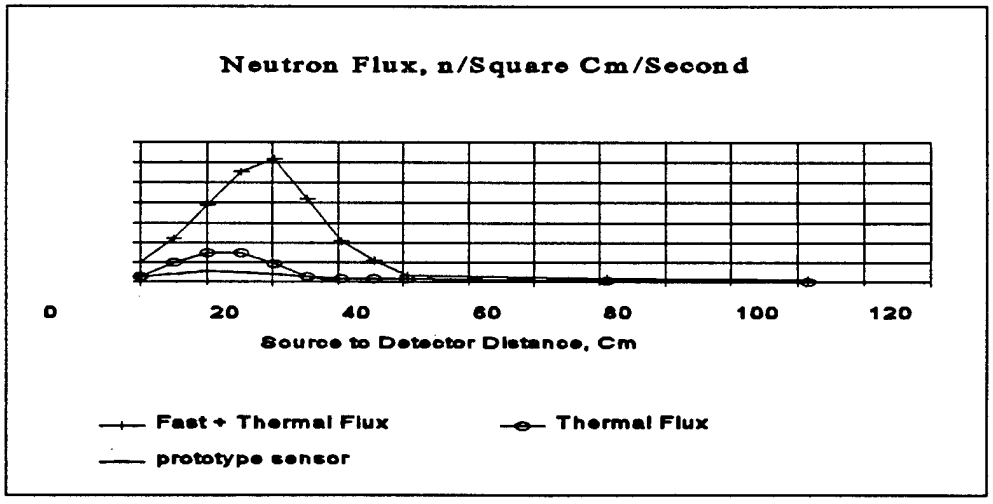

Figure 6-5. Response of Commercial Calibrated Survey Meters and the Prototype Monitor to Neutrons From an Am-Be Source.

Table 6-4. Air Neutron Measurements.

Distance Away From Plane Tangent To Detector Surface, Cms	Polymer Based Sensor Undoped Polyacetylene, Total Counts(Signal-Noise)/5 Minutes	Fast Plus Thermal Neutron Counter, CPM	Thermal Neutron Counter(nv th), CPM
25	.0.13	10.3	4.65
20	0.13	18.8	9.6
15	1.6	28.5	13.06
10	3.6	37.7	23
5	4.8	43.8	26.55
0	5.2	65	32

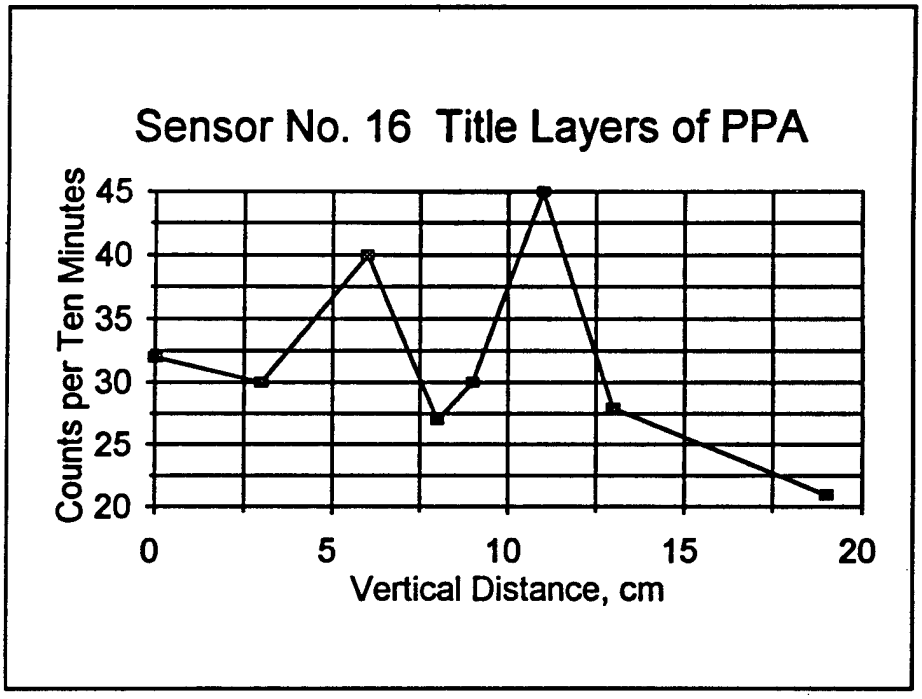

Figure 6-6. Response of Sensor With Triple Layers of Polyacetylene to the Am-Be Source.

SECTION 7

ENVIRONMENTAL TESTING OF THE PROTOTYPE NEUTRON

The neutron monitor operating temperature is limited by the operating temperature of the conductive polymer and the electronics. The electronic components were selected to operate over the full military temperature range of -55 °C to 125 C. To determine the behavior of the film under extreme conditions coupons of PA, PPY, PT were coupled to a water cooled thermionic cooler with thermal conductive epoxy and placed in an evacuated chamber and cycled between –10°C and 80 °C. The temperature of the sensor was monitored with an thermistor. Series resistance and current measurements were made on the sensors using a Keithley 610 picoammeter. None of the sensors showed evidence of failure. The conductivity changes of the sensors were calculated using the relationship

$$=\frac{L}{A}\frac{(I-I_o)}{100-(I-I_o)R},(\Omega-cm) \qquad (7.1)$$

where

L = thickness of the film

A = electrode area

I = current at 100 vdc

R = input resistance of the Keithley

I = measured current

The initial currents varied between -5 pA and 106 pA for the given sample. On the average, the conductivities decreased with decreasing temperature. From room temperature 296 K to 263K, the conductivity pA decreased from $2x10^{-11}$ down to $6x10^{-13}$ $(\Omega\text{-cm})^{-1}$.

SECTION 8

OPERATION OF THE FAST NEUTRON MONITOR

The electronics of the neutron monitor operate on two 1.5 volt Lithium batteries for 200 hours. The step power supply in the monitor is designed to provide ± 5, +3, and -98V. The sensors are self-biased and the -98 V is not in use; that is, it requires no external power source. The battery compartment can be accessed by removing four 0.635 cm 4-40 stainless steel screws. Duracell type batteries are recommended for maximum operating life.

WARNING

REMOVE BATTERIES FROM THE SPM
BEFORE SHIPMENT OR INACTIVE STORAGE
OF 30 DAYS OR MORE

The following steps must be followed for each measurement made with the monitor.

1. **Place the power switch in the "on" position (see Figure 5-3). The LCD will race due to noise.**
2. **Press the reset button. After the system has been reset, the unit now is ready to count.**
3. **Counting time must be monitored by the user.**

A 25 kΩ potentiometer is provide such that the charge preamplifier d.c. output can be zeroed (see Figure A1). Since the dark currents of the sensors varied significantly, a second potentiometer was provided such that the threshold voltage of the SCA can be adjusted.

SECTION 9
CONCLUSIONS

A set of neutron sensors and prototype monitor for use in detecting fast/thermal neurons was designed and built. The primary component of the prototype neutron monitor is the conductive polymer sensor. Isotropic and directionally sensitive sensors were tested using monoenergetic 14 MeV neutrons and an Am-Be sealed neutron source. Polyacetylene, polythrophene and polypyrrole as the active material were exposed to this wide range of neutron energies. For high energy 14 MeV neutrons the polyaceylene film material had an estimated sensitivity ~10^{-15} coulombs/neutron. The sensitivity of a sensor composed of polyacetylene surrounded by polyethylene was estimated to be ~400n/cm^2 for Am-Be neutrons. The results for the polypyrrolle and polyhiophene derivatives were inconclusive.

SECTION 10

REFERENCES

1. W. Price, Nuclear Radiation Detection, McGraw Hill Book Company, 2nd Ed., 1964. (UNCLASSIFIED)

2. G.F. Knoll, Radiation Detection and Measurement, John Wiley Pub., Co., New York, NY, 1979. (UNCLASSIFIED)

3. M.A. Butler, D.S. Ginley and J.W. Bryson, "Neutron Induced Conductivity in Transpolyacetylene," Appl. Phys. Lett., 48(19), May 12, 1986. (UNCLASSIFIED)

4. R.L. Pease et. al."Comparison of Proton and Neutron Carrier Removal Rates", IEEE Trans. on Nucl. Sci., Vol. NS 34, 6, Dec. 1987. (UNCLASSIFIED)

5. H.J. Buehler, "Design Curves for Predicting Fast Neutron Induced Resistivity Changes in Silicon," Proc. IEEE, 6, 1968. (UNCLASSIFIED)

6. D.R. Kanie et.al.,"High Speed Detection of Thermonuclear Neutrons with Solid State Detectors,"IEEE Trans. on Nucl. Sci., Vol. 19 (1), Feb. 1988. (UNCLASSIFIED)

7. D. Bloor, "Plastics that Conduct Electricity," New Scientist, March 4, 1982. (UNCLASSIFIED)

8. R.B. Kaner and A.G. MacDiarmid, "Plastics That Conduct Electricity", Scientific American, 1988. (UNCLASSIFIED)

9. S. Moyer, B.J., Survey Methods for Fast and High Energy Neutrons," Nucleonics, 10, No. 5 ,1952. (UNCLASSIFIED)

10, A.B. Smith, Neutron Standards and Flux Normalization, AEC Symposium Series 23, 1971. (UNCLASSIFIED)

11. F.Y. Shiraishi,. Takami, T Hashimoto and K. Hatori, "A New Type Personnel Neutron Dosimeter With Thin SI Detectors", IEEE Trans. Nucl. Sci.,Vol 35, Feb. 1988. (UNCLASSIFIED)

12. S.A. Cox, Beyerlein, R. and LeVert,F.E., "Development of An In-Core Directional Fuel motion Monitor", Conf. On Fuel and Clad Motion Diagnostics in LMFBR Safety Test Facilities, SAND76-5547, 1976. (UNCLASSIFIED)

13. Conner, J.C., R.G. Durnal, and V.G . Shaw; Nucleoncs, 11,1953. (UNCLASSIFIED)

14. LeVert, F.E. and E.L. Helminski, Literature Review and Commercial Source Evaluation of Americium-241, ORO-4333-1, 1973. (UNCLASSIFIED)

15. J.C. Davis,"Neutron-Proton Total Cross Section Measurements, 1.5 to 27.5 MeV," Neutron Standards and Flux Normalization, AEC Sym. Series , 23, Aug. 1971. (UNCLASSIFIED)

16. Y.W. Park, A.J. Heeger, M.A. Drug and A.G. MacDearmid, J. Chem. Phys. 73, 1980. (UNCLASSIFIED)

17. G. Paasch, Synthetic Metals, 45, 1991. (UNCLASSIFIED)

18. Yin Fang, Show-An Chen and M. Chu, Synthetic Metals, 45, 1992. (UNCLASSIFIED)

APPENDIX A
SCHEMATIC DESIGNS

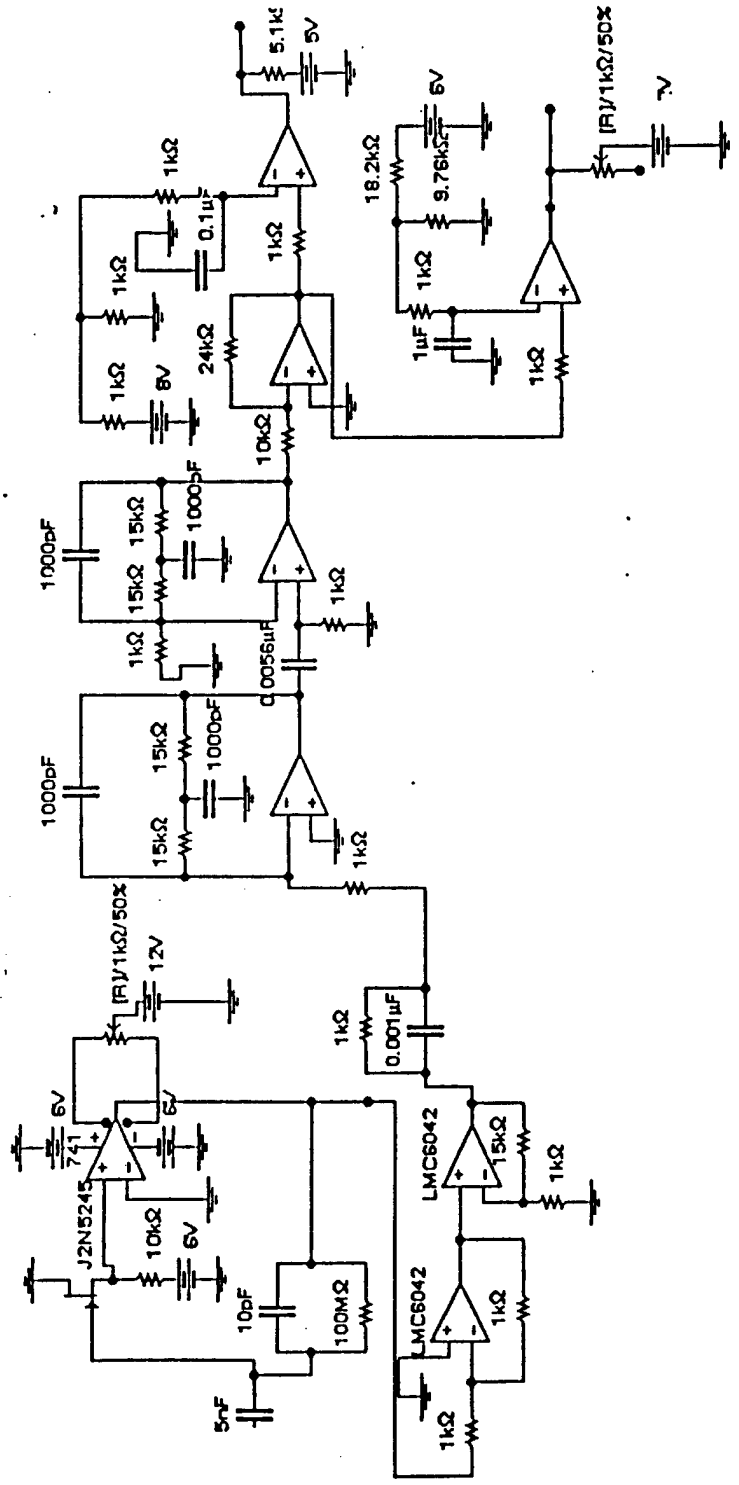

Figure A-1. Schematic of Preamplifier, Pulse Shaping Single Channel Analyzer.

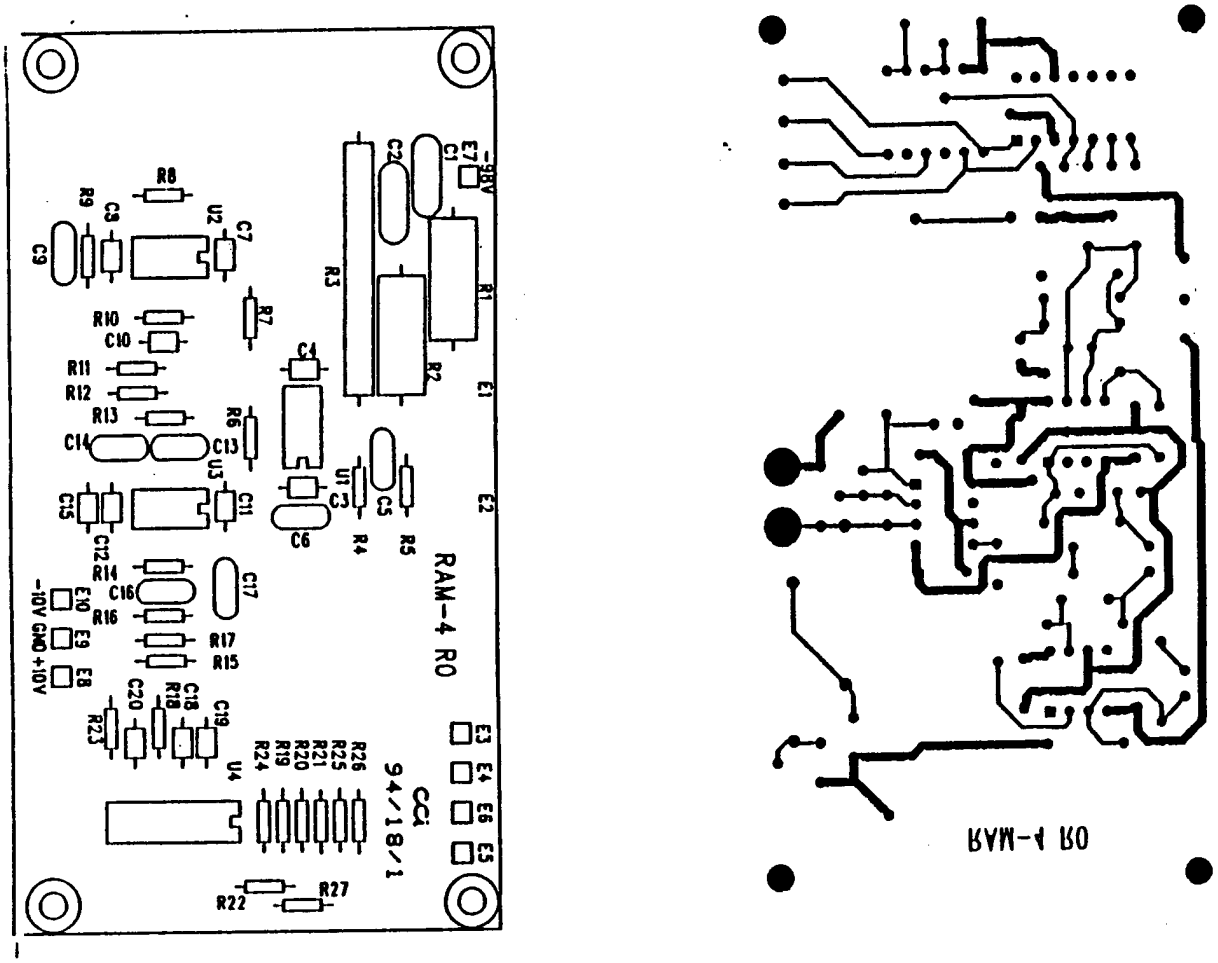

Figure A-2. Parts placement.

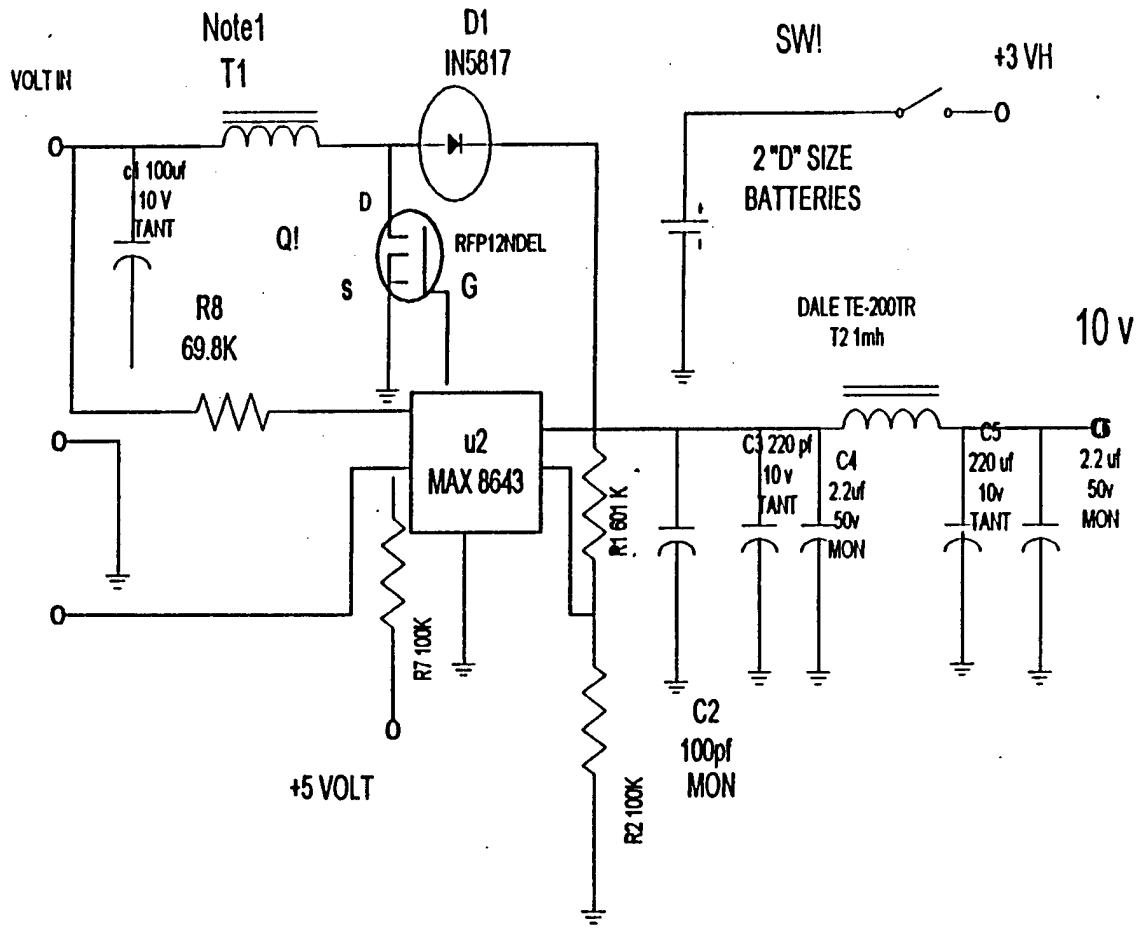

Figure A-3. Voltage Multiplier.

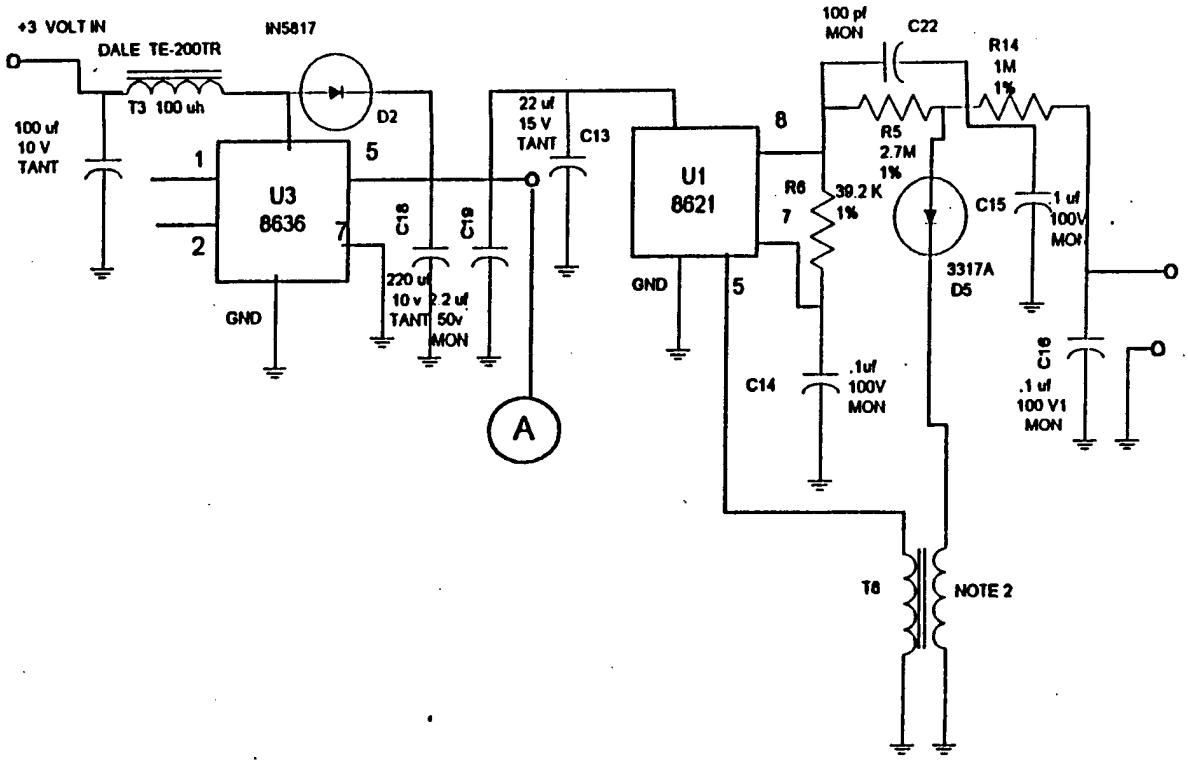

Figure A-3. Voltage Multiplier. (Continued)

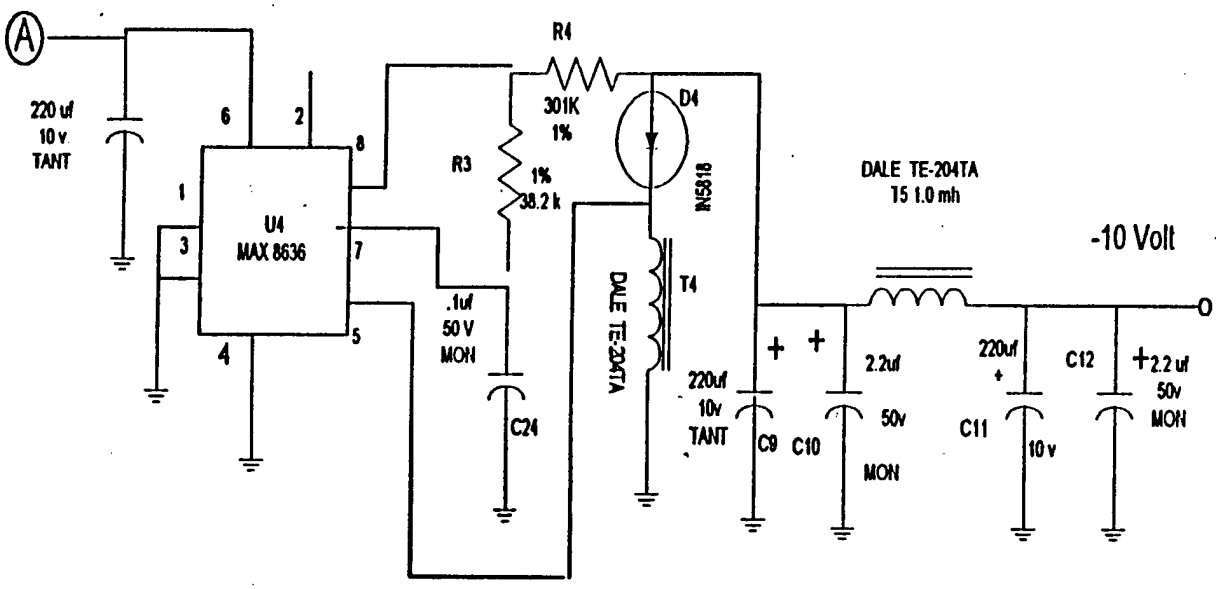

Note 1: 7.5 Turns of # 20 Enameled Wire

Note 2. PRI: 30 Turns #36 Enameled Wire.

Note 3. All Resistors RNC55 Unless otherwise Noted.

Figure A-3. Voltage Multiplier. (Continued)

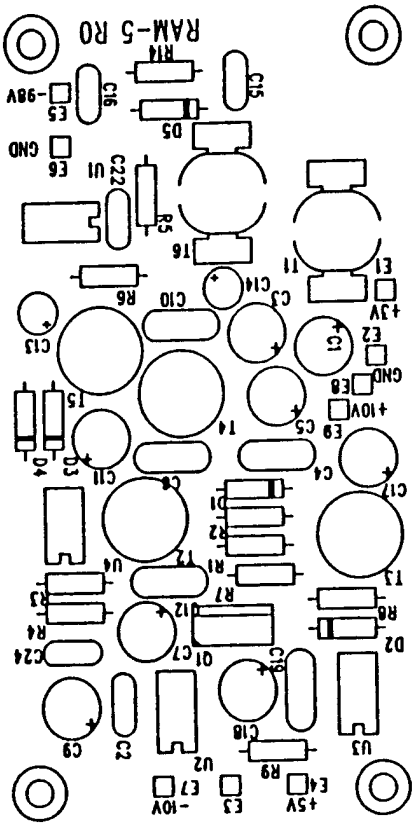

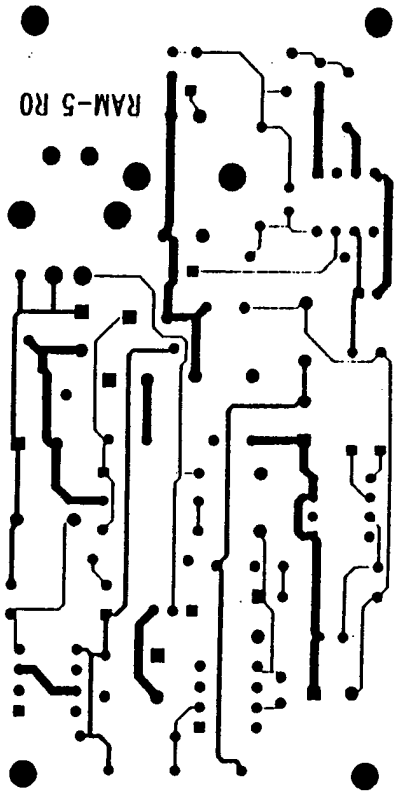

Figure A-4. Parts placement.

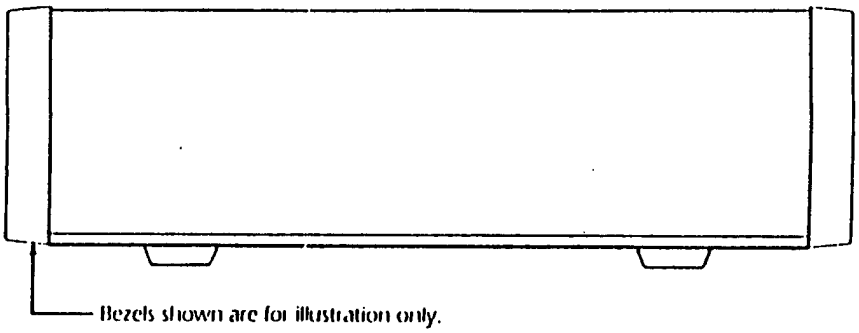

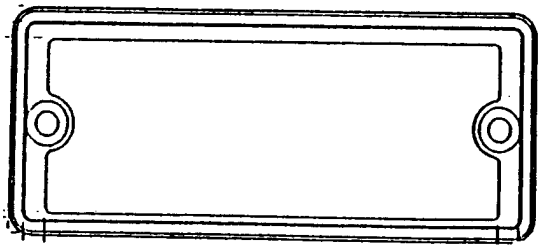

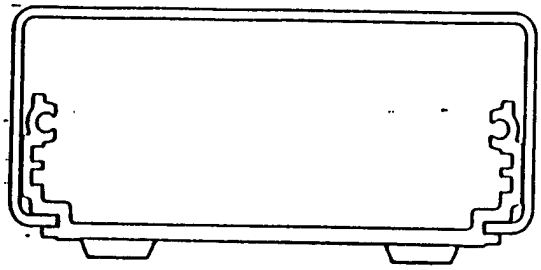

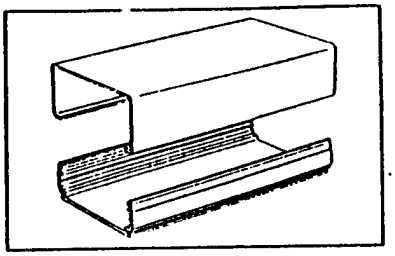

End Configuration 1:
End Panel/Bezel

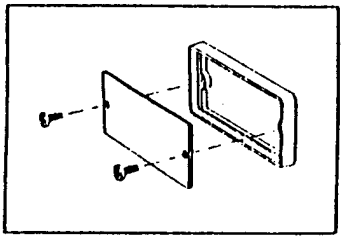

Figure A-5. Neutron enclosure mechanical.

OTTOTEK
DIVISION OF

FREQUENCY/TIMER/COUNTER
4 Digit Multi-Purpose LCD Counter
"Flat Pack" No Panel Cut Out Required
(NEMA 12 or NEMA 4)
"Naked" Panel Mount for OEMs

MODEL 522

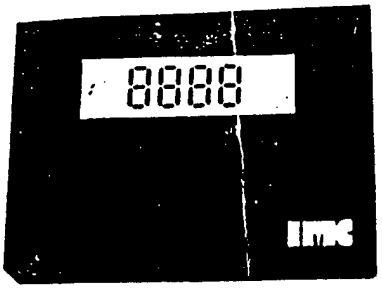

FLAT PACK

Features
- No Panel Cut-Out Required
- Elapsed Timer
- Start/Stop Timer
- Latched Overflow Indication
- High Contrast LCD
- 0.5" LCD

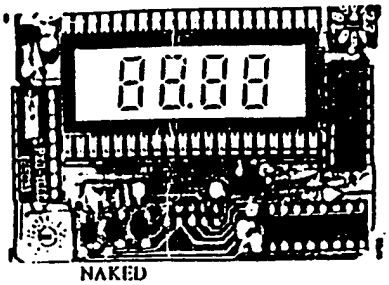

NAKED

DESCRIPTION: The 522 can be used as a frequency meter, timer or counter. In the Frequency Mode and Timer Mode, the time base is selected by two microswitches. SW2 selects one of eight primary frequencies. The other switch (SW1) divides the selected primary frequency from 1 to 10 million in steps of 10. (See table.) In the Timer Mode, it can time either a pulse duration or time duration of two pulses (Start/Stop). In the counter mode, it will accumulate any pulse from 1 Volt to 150 Volts in Amplitude at up to 200KHz.

CONTROL INPUTS: Inputs such as Reset, Counter Hold and Display Hold make it ideal for basic counting.

FLAT PACK style requires no panel cut out. Just drill a 10mm (3/8") Ø hole, pass the wires through, attach the provided double-sided tape (to prevent rotation), align the flat pack, tighten the nut and make connections to the wires. No connector or tools required! And no behind the panel space needed! The case is red acrylic and NEMA 4 options include a panel gasket and the adjustment plugs are ommitted to provide a water tight seal.

The NAKED PANEL MOUNT style is instruments on a board and mount from behind the panel. An optional bezel and filter (clear) are available to enhance your panel and give the proprietary look. The Panel Mount has a 10 pin header for flat ribbon connector.

POWER SUPPLIES: When required and ordered will be externally mounted. Two types are available, the "Open Frame" style accepts 120/240VAC and delivers 5VDC @ up to 400mADC. The "Power Pack" is a wall plug in module available only for 120VAC input and delivers 5VDC at up to 100mADC.

SPECIFICATIONS AT 25°C

Display	0.5" 9999
Overflow	Latched & Indicated by Colon
Power	5VDC ±5% at 5 mA
Inputs	TTL/CMOS Sine, Square, Triangular to 150V Peak
Frequency Responses (10-90%)	DC to 1MHz
Operating Temperature	-10 to +55°C
Storage Temperature	-20 to +60°C
Frequency Stability	±.015%
Aging	10 PPM/Yr.
Cal. Tolerance	±100 PPM

TERMINAL DESCRIPTION

1	White	**RUN/STOP:** In the timer mode, the 522 will measure the elapsed time between two positive going pulses at this terminal.
2	Blue	**COUNT-IN:** In the timer mode, connect to 7/Orange. In frequency/counter modes, connect the + input to it.
3	Violet	**COUNTER HOLD:** Normally connected to VCC. To hold the counter, or when using the run/stop function, ground it.
4	Red	**VCC:** Connect to 5VDC ±5% capable of supplying 5mA.
5	Green	**DISPLAY HOLD IN:** In the frequency mode, connect to 9/brown. In timer/counter mode, the 522 will hold when left open. Connect to ground for normal operation.
6	Black	**GROUND:** VCC return path and - input.
7	Orange	**FREQUENCY OUT:** Selected time base output. Connect to 2/blue for timer mode operation.
8	Yellow	**RESET IN:** To reset counter/timer, connect to ground 6/black. In frequency mode, connect to pin 10/gray.
9	Brown	**DISPLAY HOLD-OUT:** Leave open in counter timer mode. Connect to 5/green in frequency mode.
10	Gray	**RESET OUT:** Leave open in counter/timer mode; connect to 8/yellow in frequency mode.

ORDERING INFORMATION (9-91)

NOTE: As of this date, the display height has been increased from 0.35" to 0.5".

MODEL 5 2 2 - - - -

FUNCTION
- 5 ..... Counter
- 6 ..... Ctr/Timer/Freq

MOUNTING STYLE
- 0 ..... Flat Pack/Wires
- 1 .. NEMA 4 Flat Pack/Wires
- 8 ..... 8 Panel Mount

BEZEL & FILTER
- 0 ..... None
- 1 ..... Included

POWER INPUT
- 0 ..... 5VDC
- 1 ..... Open Frame 120/240VAC
- 2 ..... Power Pack 120 VAC

Mating Connector Included

TIME BASE SELECTION

SWITCH "1" SELECTION

SWITCH "2" SELECTION	0	1	2	3	4	5	6	7	8	9
0	N/U	100KHZ	10KHZ	1KHZ	100HZ	10HZ	1HZ	1/10HZ	SAME FUNCTION AS SW "2" ZERO	
1	100KHZ	10KHZ	1KHZ	100HZ	10HZ	1HZ	1/10HZ	1/100HZ		
2	N/U	50KHZ	5KHZ	500HZ	50HZ	5HZ	0.5HZ	0.05HZ		
3	N/U	33.3KHZ	3.333KHZ	333HZ	33.3HZ	3.33HZ	0.333HZ	0.033HZ		
4	N/U	25KHZ	2.5KHZ	250HZ	25HZ	2.5HZ	0.25HZ	0.025HZ		
5	200KHZ	20KHZ	2KHZ	200HZ	20HZ	2HZ	0.2HZ	0.02HZ		
6	166.6KHZ	16.6KHZ	1.66KHZ	166HZ	16.6HZ	1.66HZ	0.166HZ	0.016HZ		
7	83.3KHZ	8.33KHZ	833.3HZ	83.3HZ	8.33HZ	0.83HZ	0.083HZ	0.008HZ		
8	SAME FUNCTION AS SW "8" ZERO									
9	SAME FUNCTION AS SW "8" ONE									

SAME FUNCTION AS SW "1" ZERO

Figure A-6. KEMP 33001D

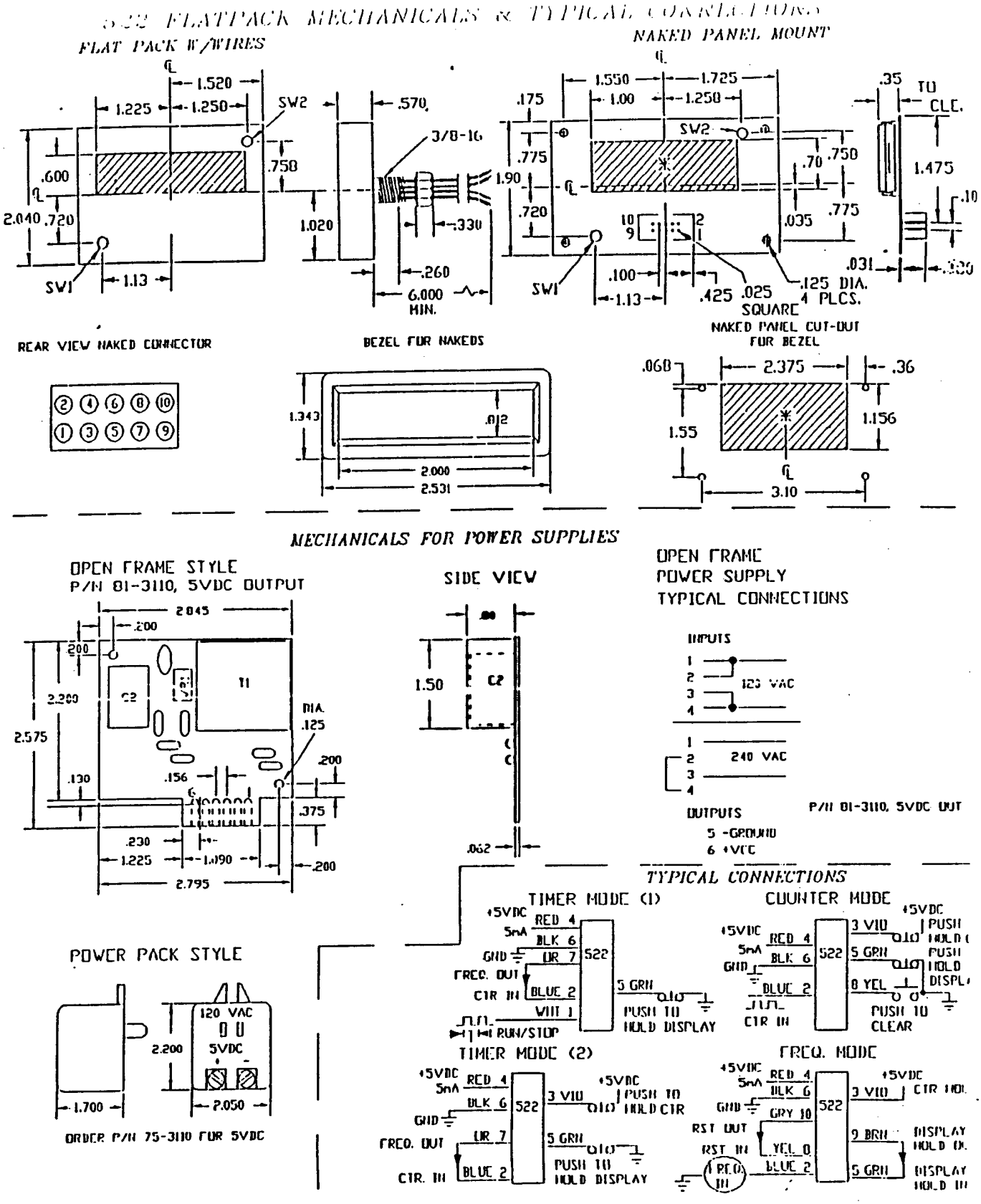

Figure A-7. LCD Counter.

Table A-1. Parts list for preamplifier, pulse sloping circuits and single channel analyzer of Figure A-1.

Quantity	Components	Properties
1	Capacitor	Capacitance: 1 microfarad
1	Capacitor	Capacitance: 1000 microfarads
4	Capacitor	Capacitance: 10 picofarads
1	Capacitor	Capacitance: 5 nanofarads
1	Capacitor	Capacitance: 0.1 microfarads
1	Capacitor	Capacitance: 0.001 microfarads
1	Capacitor	Capacitance: 0.0056 microfarads
1	N-Channel JFET	J2N5245
1	Opamp	LF351
3	Opamp	LM660
1	Potentiometer	25 kilohms
1	Potentiometer	50 kilohms
2	Resistor	Resistance: 10 kilohms
1	Resistor	Resistance: 24 kilohms
1	Resistor	Resistance: 100 megaohms
5	Resistor	Resistance: 15 kilohms
1	Resistor	Resistance: 9.76 kilohms
1	Resistor	Resistance: 18.2 kilohms
13	Resistor	Resistance: 1 kilohms
1	Resistor	Resistance: 5.1 kilohms
5	Voltage Source	Voltage: 6 volts
1	Voltage Source	Voltage: 5 volts
2	Voltage Source	

Table A-2. Parts list for voltage multiplier of Figure 3.

Quantity	Components	Properties
1	Capacitor	Capacitance: 22 microfarads
5	Capacitor	Capacitance: 2.2 microfarads
2	Capacitor	Capacitance: 100 picofarads
2	Capacitor	Capacitance: 100 microfarads
5	Capacitor	Capacitance: 220 microfarads
3	Capacitor	Capacitance: 0.1 microfarads
2	Diode	IN5817
1	Diode	IN5818
1	Diode	3317A
3	Inductor	DALE TE-200TR
2	Inductor	DALE TE-204TA
2	Integrated Circuit	MAX 8636
1	Integrated Circuit	MAX 8621
1	Integrated Circuit	MAX 8643
1	N-Channel JFET	RFP12NDEL
2	Resistor	Resistance: 100 kilohms
1	Resistor	Resistance: 601 kilohms
1	Resistor	Resistance: 1 kilohm
1	Resistor	Resistance: 38.2 kilohms
1	Resistor	Resistance: 301 kilohms
1	Resistor	Resistance: 2.7 megaohms
1	Resistor	Resistance: 39.2 kilohms
1	Time-Delay Switch	

Table A-2. Parts for voltage multiplier of Figure 3. (Continued)

Quantity	Components	Properties
1	Transformer	Ideal
2	Voltage Source	3V
1	Voltage Source	-10V
1	Voltage Source	10V
1	Voltage Source	-10V

Appendix B
Acronyms

Nomenclature

GaAs	Gallium Arsenide
MeV	Million electron volt
mm	millimeter
s	second
keV	kiloelectron volt
eV	electron volt
mrem	milliroentgen
FET	field-effect-transistor
LCD	liquid crystal display
SCA	single channel analyzer
ms	millisecond
CMOS IC	complementary metal oxide semiconductor
HV	high voltage
D-T	deuterium-tritium
n-p	neutron-proton
cm	centimeter
Ω	ohn
n	neutron
pf	picofarads
PCB	printed circuit board
RMS	root mean square
SB	surface barrier
PA	picoamperes
nf	nanofarads
MHz	megahertz
μm	micrometer
PT	polythiophene
PA	polyacetylene

DISTRIBUTION LIST
DSWA TR-96-81

DEPARTMENT OF DEFENSE

ARMED FORCES RADIOBIOLOGY RSCH INST
ATTN: AFFRI-DEPT OF RAD BIOCHEMISTRY
ATTN: BHS
ATTN: DIRECTOR
ATTN: EXH
ATTN: MRA
ATTN: PHY, M. WHITNALL
ATTN: RSD
ATTN: SCIENTIFIC DIRECTOR
ATTN: TECHNICAL LIBRARY

ASSISTANT SECRETARY OF DEFENSE
ATTN: NUC FORCES & ARMS CONTROL PLCY

DEFENSE INTELLIGENCE AGENCY
5 CY ATTN: DB-4, RSCH RESOURCES DIV
ATTN: DB-6B
ATTN: DB-6E
ATTN: DN
ATTN: DT
ATTN: OFFICE OF SECURITY
ATTN: OS
ATTN: TWJ

DEFENSE INTELLIGENCE COLLEGE
ATTN: DIC/RTS-2
ATTN: DIC/2C

DEFENSE SPECIAL WEAPONS AGENCY
ATTN: OPO
ATTN: OPS
2 CY ATTN: TRC
ATTN: WE, C MCFARLAND
ATTN: WEL
5 CY ATTN: WEP

DEFENSE TECHNICAL INFORMATION
2 CY ATTN: DTIC/OCP

FC DEFENSE SPECIAL WEAPONS AGENCY
ATTN: FCTO
2 CY ATTN: TTV 3416TH TTSQ

NATIONAL DEFENSE UNIVERSITY
ATTN: ICAF, TECH LIB
ATTN: NWCLB-CR
ATTN: STOP 315, LIBRARY
ATTN: STRAT CONCEPTS DIV CTR

OFFICE OF THE SEC OF DEFENSE
ATTN: DOCUMENT CONTROL

OASD (C3I)
ATTN: DUSP/P
ATTN: USD/P

TECHNICAL RESOURCES CENTER
ATTN: JNGO

U S EUROPEAN COMMAND
ATTN: ECJ-3
ATTN: ECJ2-O-T
ATTN: ECJ5-N, NUC BRANCH
ATTN: ECJ5D

U S EUROPEAN COMMAND/ECJ-6-DT
ATTN: ECJ-6

USSTRATCOM/J531T
ATTN: J-521

DEPARTMENT OF THE ARMY

ARMY RESEARCH LABORATORIES
ATTN: TECH LIB

COMBAT MATERIAL EVAL ELEMENT
ATTN: SECURITY ANALYST

DEP CH OF STAFF FOR OPS & PLANS
ATTN: DAMO-SWN
ATTN: DAMO-ZXA

U S ARMY WAR COLLEGE
ATTN: CENTER FOR STRATEGIC LEADERSHIP
ATTN: LIBRARY

NUCLEAR EFFECTS DIVISION
ATTN: STEWS-NE-T

TEXCOM
ATTN: CSTE-TEC-TP, D PACE

U S ARMY AIR DEFENSE ARTILLERY SCHOOL
ATTN: COMMANDANT

U S ARMY ARMOR SCHOOL
ATTN: ATSB-CTD

U S ARMY CHEMICAL SCHOOL
ATTN: CARL FRAKER

U S ARMY COMBAT SYS TEST ACTIVITY
ATTN: CSTA-RSAD, JOHN GERDES
ATTN: MIKE STANKA

U S ARMY COMD & GENERAL STAFF COLLEGE
ATTN: ATZL-SWJ-CA
ATTN: ATZL-SWT-A

U S ARMY CONCEPTS ANALYSIS AGENCY
ATTN: TECHNICAL LIBRARY

U S ARMY FIELD ARTILLERY SCHOOL
ATTN: ATSF-CD

U S ARMY FORCES COMMAND
ATTN: AF-OPTS

U S ARMY INFANTRY CENTER
ATTN: ATSH-CD-CSO

U S ARMY ITAC
ATTN: IAX-Z

U S ARMY GROUND INTELLIGENCE CENTER
ATTN: IANGIC-RMT, C WARD

U S ARMY NUCLEAR & CHEMICAL AGENCY
ATTN: MONA-NU, CPT UMEND

U S ARMY RESEARCH LAB
ATTN: AMSRL-SL-B, DR KLOPCIC
ATTN: AMSRL-SL-BS, E DAVIS
ATTN: SLCBR-D
ATTN: SLCBR-DD-T, TECH LIB
ATTN: SLCBR-TB

U S ARMY RESEARCH LABORATORY
ATTN: DIRECTOR
ATTN: DR D HODGE

U S ARMY TEST & EVALUATION COMMAND
ATTN: STECS-NE (70)

U S ARMY VULNERABILITY/LETHALITY
ASSESSMENT MANAGEMENT OFFICE
ATTN: AMSLC-VL-NE, DR J FEENEY

U S MILITARY ACADEMY
ATTN: DEPT OF BEHAVORIAL SCI & LEADERSHIP
ATTN: DEPT OF PHYSICS, LTC D FRENIER
ATTN: SCIENCE RESEARCH LAB

U S ARMY MATERIAL SYS ANALYSIS ACTVY
ATTN: DRXSY-DS

U S ARMY MEDICAL RESEARCH & DEV CMD
ATTN: SGRD-PLE

U S ARMY MODEL IMPROVEMENT STUDY
MANAGEMENT AGENCY
ATTN: SFUS-MIS, E VISCO

WALTER REED ARMY MEDICAL CENTER
ATTN: G RIPPLE
ATTN: SLRD-UWI-A, DR. HEGGE, WRAIR

DEPARTMENT OF THE NAVY

MARINE CORPS
ATTN: CODE PPO
ATTN: PSI, G RASP

NAVAL RESEARCH LABORATORY
ATTN: CODE 1240
ATTN: CODE 5227 RESEARCH REPORT

NAVAL WAR COLLEGE
ATTN: CODE E-11
ATTN: CTR FOR NAV WARFARE STUDIES
ATTN: DOCUMENT CONTROL
ATTN: LIBRARY
ATTN: STRATEGY DEPT

NUCLEAR WEAPONS TNG GROUP, ATLANTIC
ATTN: CODE 222

OFFICE OF CHIEF NAVAL OPERATIONS
ATTN: N 51
ATTN: NIS-22
ATTN: NOP 50, AVN PLNS & RQMNTS DEV
ATTN: NOP 603
ATTN: NUC AFFAIRS & INT'L NEGOT BR (N514)
ATTN: N455

OFFICE OF NAVAL INTELLIGENCE
ATTN: NTIC-DA30

OPERATIONAL TEST & EVALUATION FORCE
ATTN: COMMANDER

DEPUTY CH OF STAFF PLANS, POLICY AND OPS
ATTN: CODE-P
ATTN: CODE-POC-30

DEPARTMENT OF THE AIR FORCE

AIR UNIVERSITY
ATTN: STRATEGIC STUDIES

AIR UNIVERSITY LIBRARY
ATTN: AUL-LSE
ATTN: LIBRARY

ARMSTRONG LABORATORY
ATTN: AL/CFBE, DR F S KNOX

STUDIES AND ANALYSES AGENCY
ATTN: AFSAA/SAMI

DEPUTY CHIEF OF STAFF FOR PLANS & OPS
ATTN: AFXOOSS

HQ ACC/XP-JSG
ATTN: ACC/XP-JSG

HQ USAFA/DFSELD
ATTN: LIBRARY

HQ 497 IG/INOT
ATTN: INT

NATIONAL AIR INTELLIGENCE CENTER
ATTN: NAIC/GTA

DEPARTMENT OF ENERGY

OAK RIDGE OPERATION
ATTN: DR T JONES

OAK RIDGE NATIONAL LABORATORY
ATTN: G KEER
ATTN: J PACE
ATTN: J WHITE

LAWRENCE LIVERMORE NATIONAL LAB
ATTN: L-315, A WARSHAWSKY
ATTN: Z DIVISION LIBRARY

LOS ALAMOS NATIONAL LABORATORIES
ATTN: D STROTTMAN
ATTN: REPORT LIBRARY

SANDIA NATIONAL LABORATORIES
ATTN: TECH LIB

OTHER GOVERNMENT

CENTAL INTELLIGENCE AGENCY
ATTN: COUNTER-TERRORIST GROUP
ATTN: DIRECTOR OF SECURITY
ATTN: MEDICAL SERVICES
ATTN: NIO-T
ATTN: N10-STRATEGIC SYS

FEDERAL EMERGENCY MANAGEMENT AGENCY
ATTN: CIVIL SECURITY DIVISION
ATTN: NP-CP
ATTN: OFC OF CIVIL DEFENSE

U S DEPARTMENT OF STATE
ATTN: PM/STM

U S NUCLEAR REGULATORY COMMISSION
ATTN: DIR DIV OF SAFEGUARDS
ATTN: S YANIV

DEPARTMENT OF DEFENSE CONTRACTORS

ARES CORP
2 CY ATTN: A DEVERILL

EAI CORPORATION
ATTN: MILLARD MERSHON
ATTN: DENNIS METZ
ATTN: KRISTIN GAVLINSKI

FULTON FINDINGS
ATTN: WES FULTON

INSTITUTE FOR DEFENSE ANALYSES
ATTN: DOUGLAS SCHULTZ

JAYCOR
ATTN: CYRUS P KNOWLES

K.E.M.P. CORPORATION
2 CY ATTN: FRANCIS E LEVERT

KAMAN SCIENCES CORPORATION
ATTN: DASIAC
ATTN: DASIAC/DARE

LOCKHEED MARTIN CORPORATION
ATTN: WE-YOUNG WOO

LOGICON R AND D ASSOCIATES
ATTN: DOCUMENT CONTROL

LOGICON R AND D ASSOCIATES
ATTN: S WOODFORD

MASSACHUSETTS INSTITUTE OF TECHNOLOGY
ATTN: DUNCAN C MILLTER

MICRO ANALYSIS AND DESIGN
ATTN: N LAVINE
ATTN: R LAUGHERY
ATTN: T ROTH

PACIFIC-SIERRA RESEARCH CORP.
2 CY ATTN: G ANNO
ATTN: J BRODE

PACIFICE-SIERRA RESEARCH CORP
ATTN: D GORMLEY
2 CY ATTN: G MCCLELLAN

PSYCHOLOGICAL RESEARCH CENTER
ATTN: L GAMACHE

SCIENCE APPLICATIONS INTL CORP
ATTN: D KAUL, MS 33
ATTN: E SWICK, MS 33
ATTN: L HUNT
ATTN: R J BEYSTER, MS 47
ATTN: W WOOLSON

SCIENCE APPLICATIONS INTL CORP
ATTN: J MCGAHAN
ATTN: J PETERS
ATTN: P VERSTEEGEN
ATTN: W LAYSON

SCIENCE APPLICATION INTL CORP
ATTN: R CRAVER

TECHNICO SOUTHWEST INC
ATTN: S LEVIN

TRW INC.
ATTN: T.I.C., S/1930

TRW OGDEN ENGINEERING OPERATIONS
ATTN: D C RICH

TRW S.I.G.
ATTN: DR BRUCE WILSON

UNIVERSITY OF CINICINNATI MEDICAL CENTER
ATTN: E SILVERSTEIN

UNIFORMED SVCS UNIV OF THE HLTH SCI
ATTN: EHS, LTC JOHN L BLISS

UNIV OF ILLINOIS-WILLIARD AIRPORT
ATTN: H L TAYLOR